Organic & Biomolecular Chemistry

ROYAL SOCIETY OF CHEMISTRY

PAPER

View Article Online
View Journal | View Issue

Cite this: *Org. Biomol. Chem.*, 2024, **22**, 767

Switching the three-component Biginelli-like reaction conditions for the regioselective synthesis of new 2-amino[1,2,4]triazolo[1,5-*a*]pyrimidines†

Martina Pacetti, ‡[a] Maria Chiara Pismataro, ‡[a] Tommaso Felicetti, *[a] Federica Giammarino, [b] Anna Bonomini, [c] Matteo Tiecco, [d] Chiara Bertagnin, [c] Maria Letizia Barreca, [a] Raimondo Germani, [e] Violetta Cecchetti, [a] Ilaria Vicenti, [b] Oriana Tabarrini, [a] Maurizio Zazzi, [b] Arianna Loregian [c] and Serena Massari [a]

Among the eight different triazolopyrimidine isomers existing in nature, 1,2,4-triazolo[1,5-*a*]pyrimidine (TZP) is one of the most studied and used isomers in medicinal chemistry. For some years, our group has been involved in developing regioselective one-pot procedures for the synthesis of 2-amino-7-aryl-5-methyl- and 2-amino-5-aryl-7-methyl-TZPs of interest in the preparation of antiviral agents. In this work, taking advantage of a Biginelli-like multicomponent reaction (MCR), we report the identification of finely tunable conditions to regioselectively synthesize C-6 ester-substituted amino-TZP analogues, both in dihydro and oxidized forms. Indeed, the use of mild acidic conditions is strongly directed toward the regioselective synthesis of 5-aryl-7-methyl C-6-substituted TZP analogues, while the use of neutral ionic liquids shifted the regioselectivity towards 7-aryl-5-methyl derivatives. In addition, the novel synthesized scaffolds were functionalized at the C-2 position and evaluated for their antiviral activity against RNA viruses (influenza virus, flaviviruses, and SARS-CoV-2). Compounds **25** and **26** emerged as promising anti-flavivirus agents, showing activity in the low micromolar range.

Received 16th November 2023,
Accepted 19th December 2023

DOI: 10.1039/d3ob01861j

rsc.li/obc

Introduction

Triazolopyrimidine represents a privileged structure in agrochemical and medicinal chemistry, with numerous derivatives that have found applications in several biological and medical fields.[1–3] Among the eight different triazolopyrimidine isomers existing in nature, [1,2,4]triazolo[1,5-*a*]pyrimidine (hereafter abbreviated TZP for convenience) has been the most studied and used isomer in medicinal chemistry, especially to design and synthesize novel anti-infective agents.[3–5] However, recent articles and reviews show the potential of this nucleus to develop compounds endowed with several biological activities, also taking advantage of its favourable pharmacokinetic properties.[1,3,4,6]

For some years, our group has been involved in the synthesis of TZP-based compounds as inhibitors of RNA viruses, mainly as an anti-influenza virus (IV) agents able to inhibit RNA-dependent RNA polymerase (RdRP) PA–PB1 subunits interaction.[7–10] Starting from the hit compound **1** (Scheme 1a), several compounds were designed and synthesized by exploring the role of the C-2 amide substituent and modifying the TZP nucleus by: (i) aromatization of the 4,7-dihydro-[1,2,4]triazolo[1,5-*a*]pyrimidine core, (ii) exchange of 5-methyl and 7-phenyl moieties, (iii) inversion of the C-2 amide link, (iv) decoration of the C-5/C-7 phenyl ring with different substituents, (v) removal of the methyl moiety while maintaining only a phenyl ring at the C-7, C-5, or C-6 position, and (vi) replacement of the C-7 methyl group by a hydroxyl group (Scheme 1a). These modifications led to the identification of compounds that exhibited an improved ability to inhibit PA–

[a]*Department of Pharmaceutical Sciences, University of Perugia, 06123 Perugia, Italy. E-mail: tommaso.felicetti@unipg.it; Tel: +39 075-5852185*
[b]*Department of Medical Biotechnologies, University of Siena, 53100 Siena, Italy*
[c]*Department of Molecular Medicine, University of Padua, 35121 Padua, Italy*
[d]*Chemistry Interdisciplinary Project (ChIP), School of Pharmacy, University of Camerino, 62032 Camerino, MC, Italy*
[e]*Department of Chemistry, Biology and Biotechnology, University of Perugia, 06123 Perugia, Italy*

†Electronic supplementary information (ESI) available: Superposition of ^{1}H NMR and ^{13}C NMR spectra of compounds **10** and **11**, and **8** and **9**. NOESY spectra of compounds **10** and **11**. ^{13}C NMR chemical shifts (δ, ppm) of compounds **8–11** and **16–19**. Optimization of reaction conditions for compounds **8–11**. Plausible reaction mechanisms for the formation of compounds **10** and **11**. Anti-DENV-2, WNV, and SARS-CoV-2 activity, and cytotoxicity of TZP derivatives **23–30**. ^{1}H NMR and ^{13}C NMR spectra for compounds **8–11**, **16–19** and **23–30**. HRMS analyses of compounds **8–11** and **23–30**. HPLC chromatograms of compounds **23–30**. FT-IR spectra for compounds **8–11**. See DOI: https://doi.org/10.1039/d3ob01861j

‡Co-first authors.

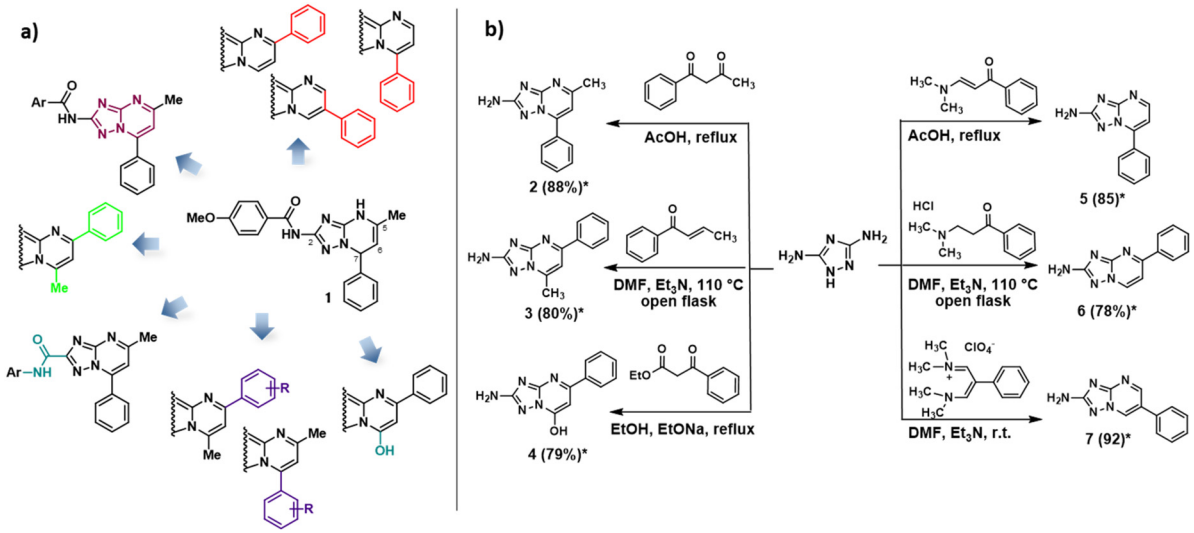

Scheme 1 (a) Structural modifications performed on the TZP core during the optimization of anti-IV hit compound **1**. (b) Chemical procedures previously developed by us for the synthesis of 2-amino-TZP compounds **2–7**. *Isolated yield.

PB1 interaction with respect to **1** and, above all, acquired anti-IV activity at non-toxic concentrations.[7,9]

During the synthesis of anti-IV TZPs, efforts were directed towards the development of one-pot procedures to directly obtain oxidized TZPs. In particular, starting from 3,5-diaminotriazole, we reported facile and efficient one-step procedures for the regioselective synthesis of 2-amino-5-methyl-7-phenyl-[1,2,4]triazolo[1,5-*a*]pyrimidines (exemplified by compound **2**),[11] 2-amino-7-methyl-5-phenyl-[1,2,4]triazolo[1,5-*a*]pyrimidines (exemplified by compound **3**),[11] 2-amino-5-phenyl-[1,2,4]triazolo[1,5-*a*]pyrimidin-7-ol **4**,[8] and 7-phenyl-, 5-phenyl-, and 6-phenyl-2-amino-[1,2,4]triazolo[1,5-*a*]pyrimidines **5–7** (Scheme 1b).[8]

Keeping our interest on TZP-based compounds as antiviral agents, in this work, we focused on the synthesis of C-5, C-6, and C-7 trisubstituted TZPs taking advantage of a Biginelli-like multicomponent reaction (MCR) for their preparation. MCRs represent a powerful approach for achieving diversity and complexity of organic compounds, reducing the number of reaction steps and the environmental impact, thus combining molecular diversity, depending on the structures of the reagents, the solvent, and the catalyst, with eco-compatibility.

Some examples of Biginelli-like reactions for the synthesis of the TZP scaffold that combine aldehydes, compounds with an active methylene group, and polyfunctional aminotriazoles have been reported in the literature (readers are directed to reviews),[3,12–16] mainly furnishing C-2 unsubstituted TZP derivatives, such as 4,5,6,7-tetrahydro-TZPs,[17] 4,7-dihydro-TZPs,[18,19] and aromatic TZP analogues[20] (Fig. 1 – general structures I–IV). Less attention has been paid to C-2-functionalized TZP derivatives, with only a few examples reporting 4,7-dihydro TZP analogues (general structure V in Fig. 1).[21–23]

Herein, we reported for the first time two Biginelli-like MCRs to obtain directly and regioselectively aromatic 2-substituted TZPs. In particular, ethyl 2-amino-5-methyl-7-phenyl-[1,2,4]triazolo[1,5-*a*]pyrimidine-6-carboxylate (**8**) and ethyl

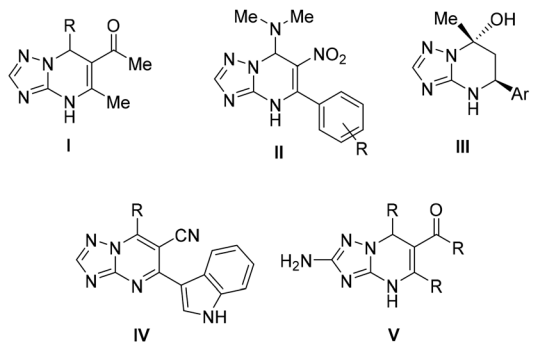

Fig. 1 Examples of functionalized dihydro, tetrahydro, and aromatic TZP derivatives (general structures **I–V**) obtained by Biginelli-like MCRs.

2-amino-7-methyl-5-phenyl-[1,2,4]triazolo[1,5-*a*]pyrimidine-6-carboxylate (**9**) (Scheme 2a) were regioselectively synthesized *via* the reaction of 3,5-diaminotriazole, benzaldehyde, and ethyl 3-oxobutanoate, under liquid ionic and acidic conditions, respectively. Moreover, the use of the same environments while changing the reaction conditions permitted us to regioselectively and efficiently obtain the dihydro analogues ethyl 2-amino-5-methyl-7-phenyl-4,7-dihydro-[1,2,4]triazolo[1,5-*a*]pyrimidine-6-carboxylate (**10**)[21] and ethyl 2-amino-7-methyl-5-phenyl-4,7-dihydro-[1,2,4]triazolo[1,5-*a*]pyrimidine-6-carboxylate (**11**) (Scheme 2a).

By taking advantage of the developed procedures, additional aromatic 2-amino-TZPs variously functionalized at the C-6 position were synthesized and used as key intermediates to be further functionalized at the C-2 position. Antiviral evaluation of the synthesized compounds (**23–30**, Scheme 2b) against IV, two flaviviruses (dengue and West Nile virus), and SARS-CoV-2 led to the identification of derivatives **25** and **26**, which showed anti-flavivirus activity in the low micromolar range.

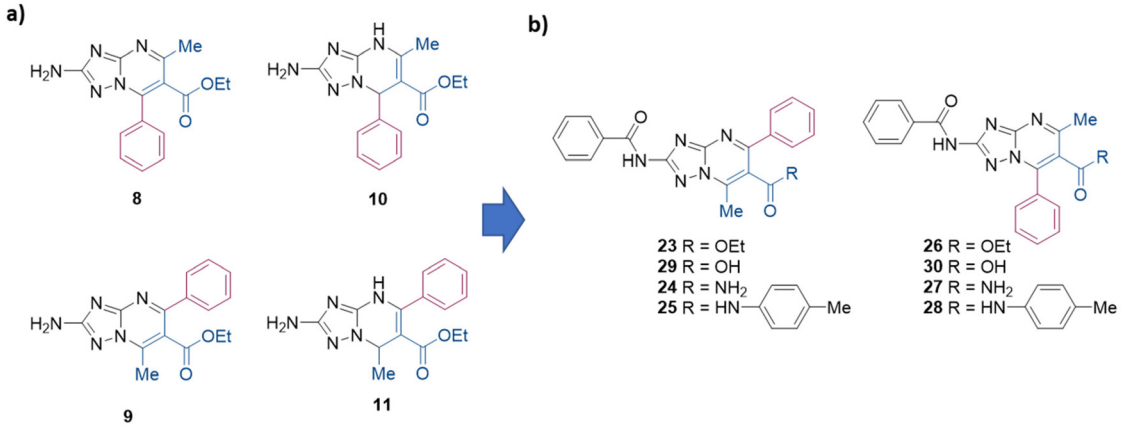

Scheme 2 (a) Structures of TZP scaffolds **8–11** regioselectively synthesized in this work. (b) Successive target compounds synthesized and evaluated as antiviral agents.

Results and discussion

Synthesis of ethyl 2-amino-[1,2,4]triazolo[1,5-*a*]pyrimidine-6-carboxylates 8–11

Two procedures have been previously reported for the synthesis of non-oxidized 5-methyl-7-phenyl-TZP **10** by Chernyshev and coworkers (Schemes 3a and b).[21,24] In the first procedure reported in 2007,[21] 3,5-diaminotriazole (**12**) (1 equiv.), benzaldehyde (**13**) (1 equiv.), and ethyl 3-oxobutanoate (**14**) (1 equiv.) were reacted in DMF at reflux for 30 min, furnishing a mixture of **10** and azomethine compound **15**, which was treated with hydrazine hydrate to give **10** in 44% yield (Scheme 3a). In the successive procedure reported in 2017,[24] the reaction of **13** and **14** in AcOH in the presence of piperidine furnished an intermediate bis-electrophile, which was then reacted with **12** yielding **10** in 71% yield (Scheme 3b).

Looking for a MCR allowing for the synthesis of compound **10** through a single step and a greener approach, we reacted **12** (1 equiv.), **13** (1 equiv.), and **14** (1 equiv.) in EtOH at reflux in the presence of citric acid (2.5 equiv.) (Scheme 3c) following a similar procedure previously reported for the synthesis of 1,4-dihydro-benzo[4,5]imidazo[1,2-*a*]pyrimidine analogues.[25] After 5 h, the reaction furnished a mixture containing **10** only in traces, while, surprisingly, the main product (albeit obtained after purification in 16% yield) was isomer **11**, as confirmed by 2D NMR (NOESY experiment), along with traces of another unknown compound (later characterized as the oxidized TZP analogue **9**).

NMR signals and NOESY correlation for compounds **10** and **11** are shown in Fig. 2, and the superposition of NMR spectra and NOESY spectra is reported in Fig. S1–S4.† The values of the main ^{13}C NMR signals are also reported in Table S1.† In the ^{1}H NMR spectrum of compound **11**, the signals of NH and H-7 are shifted upfield by 1.9 ppm and 0.5 ppm, respectively, with respect to those of isomer **10**. Moreover, in the ^{13}C NMR spectrum of compound **11**, the signals of C-5 and C-6 are shifted downfield by 7.2 and 3.4 ppm, respectively, with respect to those of **10**, while the signals of C-7 and CH_3 carbon are shifted upfield by 6.6 and 3.2 ppm, respectively. In NOESY experiments, the singlet of NH of derivative **11** (8.55 ppm) correlated with multiplets (7.21–7.34 ppm) generated by the aromatic proton of the phenyl group at the C-5 position, while the singlet of NH (10.47 ppm) of **10** correlated with the singlet (2.37 ppm) of the methyl group at the C-5 position (violet arrows in Fig. 2a, and Fig. S3 and S4†). As a confirmation, the singlet of H-7 (5.94 ppm) of derivative **10** correlated with the multiplets (7.15–7.31 ppm) generated by the aromatic proton of the phenyl group at the C-7 position (violet arrow in Fig. 2a and S3†).

At this point, compounds **10** (synthesized following the procedure reported in Scheme 3b) and **11** were oxidized by using NBS, furnishing compounds **8** and **9** in 48% and 26% yields, respectively (Scheme 3b and c). The NMR signals for compounds **8** and **9** are shown in Fig. 2 (the main ^{13}C NMR signals are also reported in Table S1†) and the superposition of NMR spectra is reported in Fig. S5 and S6.† By comparing the ^{13}C NMR spectrum of compound **9** to that of compound **8**: (i) the signals of TZP carbons C-2, C-6 and C-7 of compound **9** are all slightly shifted upfield by 0.6–0.9 ppm (C-2 = 0.9 ppm, C-6 = 0.7 ppm, and C-7 = 0.6 ppm), (ii) the signals of C-3 and C-5 are slightly shifted downfield by 0.9 and 0.2 ppm, respectively, and (iii) the signal of CH_3 carbon is shifted upfield by 8.2 ppm.

As mentioned previously, once the two oxidized isomers were obtained and characterized, we learned that the reaction reported in Scheme 3c furnished traces of oxidized compound **9**, besides compounds **10** and **11**. Based on the observation that these reaction conditions favoured the synthesis of 7-methyl-5-phenyl-TZP rather than 5-methyl-7-phenyl-TZP isomers, additional reaction conditions were further explored with the aim to regioselectively obtain the C-5 phenyl isomer derivatives **9** and **11**. In this phase, efforts were also focused on the development of a HPLC method that, through the retention time (tR), allowed us to quickly detect isomers **8–11** and their ratios (Fig. 3).

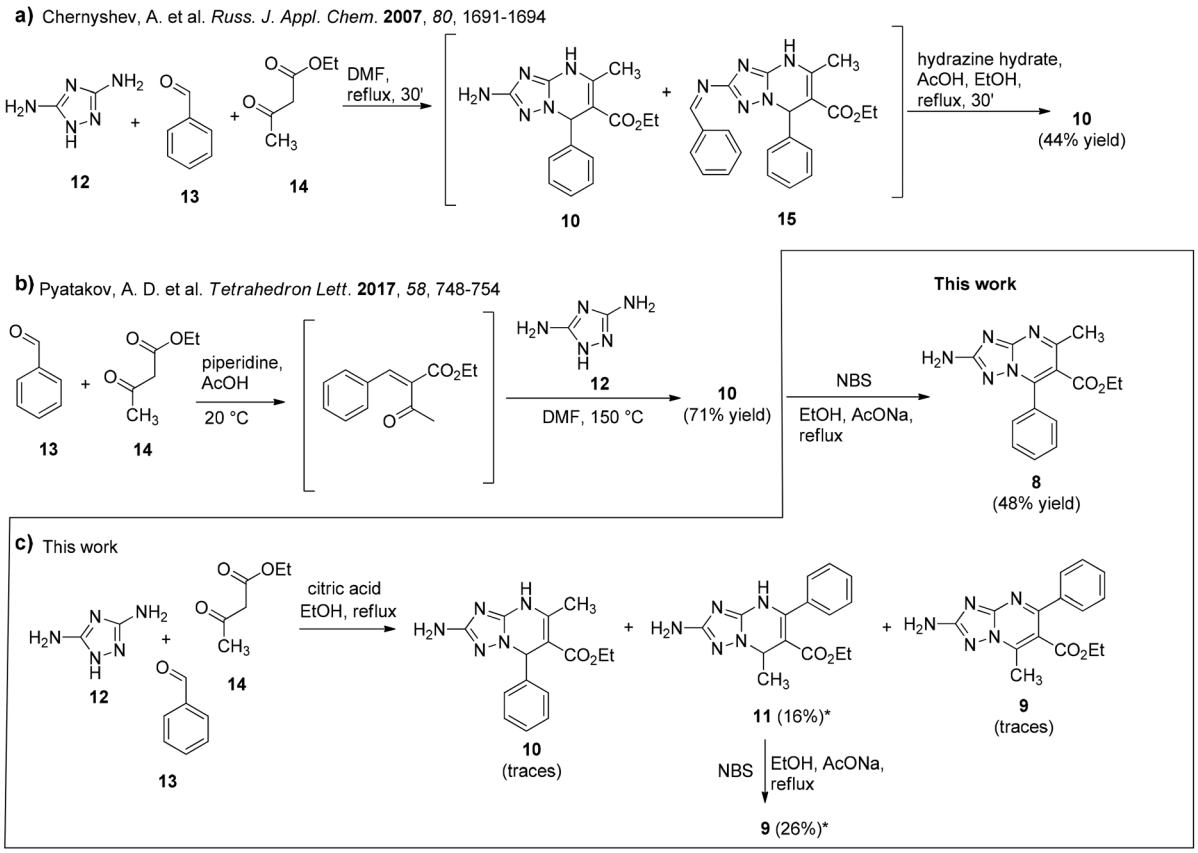

Scheme 3 (a) and (b) Known procedures for the synthesis of **10**. (b) Oxidation of **10** to aromatic TZP **8** performed in this work. (c) Synthesis of **11** *via* the MCR of 3,5-diaminotriazole (**12**), benzaldehyde (**13**) and ethyl 3-oxobutanoate (**14**), and its oxidation to compound **9**, respectively. *Isolated yield.

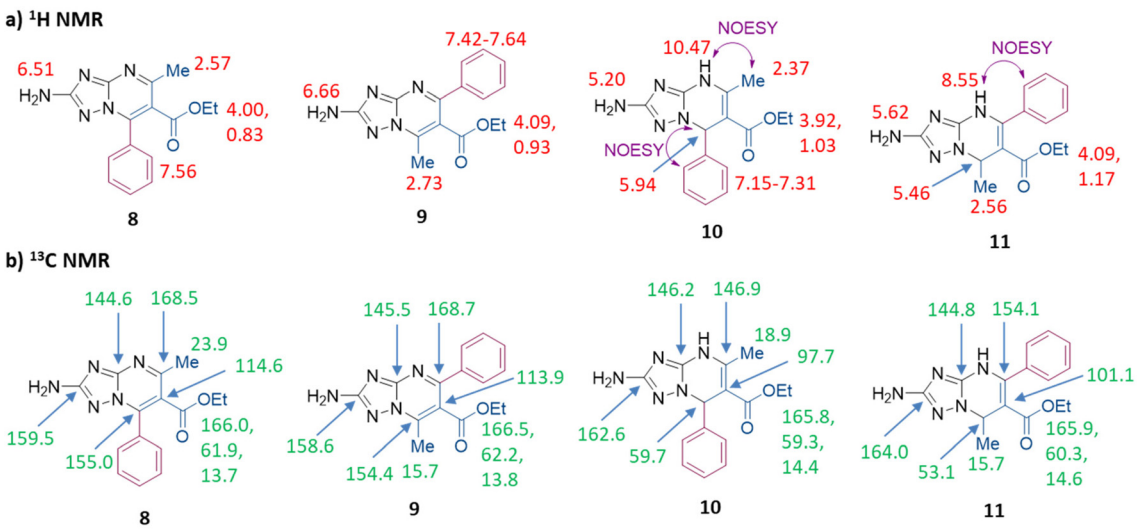

Fig. 2 (a) ^{1}H NMR and (b) ^{13}C NMR spectral characteristics (chemical shifts δ, ppm) of compounds **8–11** in DMSO and key correlation in the NOESY spectra.

The reaction of **12** (1 equiv.), **13** (1 equiv.), and **14** (1 equiv.) in EtOH at reflux in the presence of citric acid (2.5 equiv.) (Table S2,† entry 1) was repeated by increasing the equiv. of citric acid (5 equiv., entry 2) or compound **13** (1.5 equiv., entry 3), but no significant changes in the outcome of the reaction were noted. Nevertheless, only by decreasing the reaction time

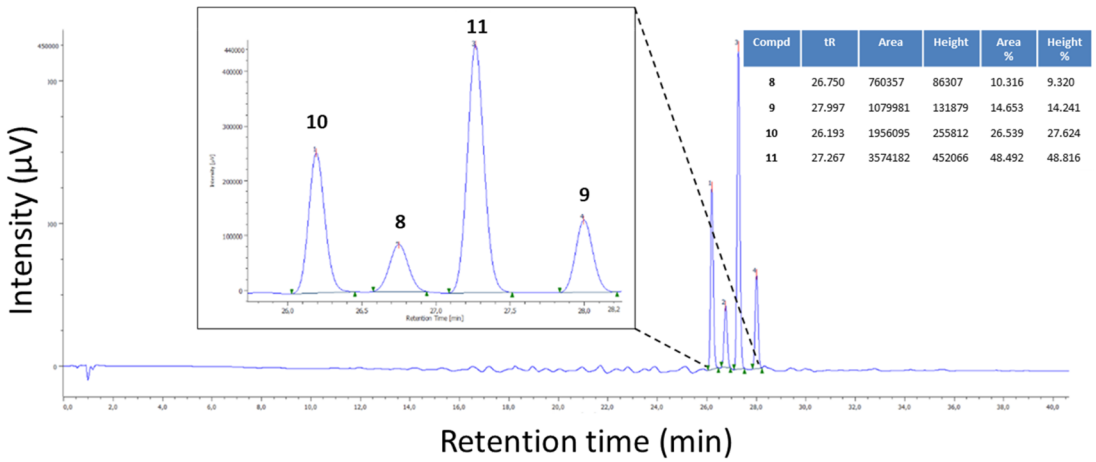

Fig. 3 Example of HPLC chromatogram of a mixture of compounds **8–11**. HPLC method: RP-C18; flow: 0.4 mL min^{-1}; 0.1% formic acid in H_2O 100% to 0.1% formic acid in H_2O 50% : CH_3CN 50% in 40 min.

from 5 h to 3.5 h (entry 4), compound **11** was regioselectively obtained in 83% yield (Table 1, entry a). Of note, the purification of compound **11** was performed by trituration of the solid in Et_2O without the involvement of chromatography. Noteworthy is the propensity of compound **11**, when solubilized in different organic solvents such as EtOAc, $CHCl_3$, or $CHCl_3$/MeOH, to spontaneously oxidize, furnishing derivative **9** in a few days at room temperature (rt), albeit not completely (about 50%). All attempts to completely convert derivative **11** into derivative **9** (solutions of **11** in different organic solvents were stirred overnight at rt, under light, or gently heated) failed. In contrast, it was stable when stored as a pure powder over time.

Searching for alternative procedures for the synthesis of compound **9** in higher yields, the reaction of **12** (1 equiv.), **13** (1 equiv.), and **14** (1 equiv.) was performed under microwave (μw) irradiation or in different solvents and/or by using different acid catalysts (Table S2,† entries 5–9). Overall, many spots were observed by TLC due to the formation of several side products. Of note, the reaction performed in THF in the presence of *para*-toluenesulfonic acid (PTSA) as the catalyst at reflux (entry 6) showed a certain degree of regioselectivity towards C-5 phenyl isomers, but after 24 h, not enough conversion from **11** to **9** was observed. Interestingly, the reaction performed in glacial acetic acid at reflux under nitrogen (entry 9) furnished compound **9** after 6 h with a certain degree of selectivity, even though several side products were formed. After purification, compound **9** was obtained in 21% yield, highlighting that the aromatic C-5 phenyl isomer can be directly achieved through a Biginelli-like MCR as a major compound.

Prompted by these results, the reaction was repeated in glacial acetic acid at reflux but in an open flask (Table S3†) in order to promote the oxidation reaction, analogously to procedures previously reported by us (Scheme 1b).[8,11] In these reactions, the effects of the reaction time, the temperature, and the equiv. of each of the starting compounds were studied.

Table 1 Best reaction conditions for the synthesis of regioisomers **8–11** [a]

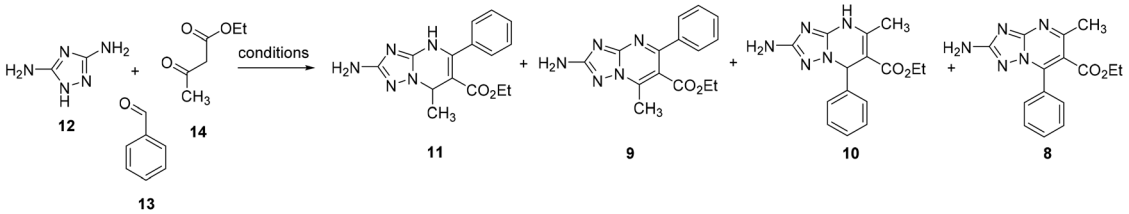

Entry	Solvent	Ratio 12 : 13 : 14	Catalyst (equiv.)	*T*°	Time (h)	% yield of **8–11**
a	EtOH	1 : 1 : 1	Citric acid (2.5)	Reflux	3.5	**11** in 83%[b]
b	AcOH	1 : 3 : 1	—	60 °C	9	**9** in 55%[b]
c	TBMA MsO	1 : 1 : 1	—	120 °C	24	**10** in 75%[b]
d	BMIM MsO	1 : 2 : 1	H_2O_2 [c]	120 °C	24	**8** in 40%[b]

[a] The reaction was performed on a 1.0 mmol scale of **12** in 3 mL of solvent. [b] Isolated yield. [c] H_2O_2 (1 mL) was added after 12 h.

As expected, performing the reaction in an open flask favoured the oxidation of **11** into **9**, accompanied by increased regioselectivity of the reaction. In particular, the best results were obtained by reacting **12** (1 equiv.), **13** (1 equiv.), and **14** (1 equiv.) in AcOH at 120 °C for 6 h (Table S3,† entry 2), with a percentage ratio of 89% for **9** and a yield of 37%. A shorter time (entry 1) did not permit a complete conversion of **11** into **9**, while at longer times (entries 3 and 4), the formation of side products increased over time. Changing the equiv. of the starting materials (entries 7–11) was in general detrimental for the regioselectivity as well as for the efficiency of the reaction, owing to the excessive presence of side products. Very minor tarring was observed instead when performing the reaction at 60 °C (entries 5 and 6), although it was detrimental for the oxidation of **11** into **9**.

Based on these results, we attempted again to perform the reaction under nitrogen (Table S4†). Thus, the reaction was repeated by evaluating the effect of the equiv. of the starting compounds, temperature, time, and/or the presence of a catalyst. The use of 2 equiv. of diaminotriazole **12** (entry 1) led to reaction tarring and a decrease in regioselectivity. On the other hand, the increase of benzaldehyde **13** (2 equiv., entries 2 and 3) furnished compound **9** as the major isomer. Of note, the best results were observed when performing the reaction at reflux (entry 2), with **9** being present with a percentage ratio of 77% (63% when the temperature was 60 °C, entry 3). According to the peak ratio, trituration using Et_2O/EtOH gave compound **9** in 51% (entry 2) and 33% (entry 3) yields.

A further increase of benzaldehyde **13** (3 equiv., entries 4–6) led to good results only by performing the reaction at 60 °C, obtaining compound **9** after 9 h with a peak ratio of 78% and an isolated yield of 55% after purification by chromatography (Table 1, entry b); higher temperatures led to a decrease in regioselectivity. On the other hand, using 2 equiv. of **14** (entries 7–9), a higher peak ratio for **9** was obtained by performing the reaction at reflux, while a large amount of **11** was observed at lower temperatures. Although a good percentage peak ratio (83%) was obtained, the conditions used for entry 9 led to several side products, likely due to the reflux temperature, as demonstrated by the low reaction yield (23%). Analogous results were obtained by combining 3 equiv. of **13** and 2 equiv. of **14** at 60 °C (entry 10), which led to a good percentage peak ratio of compound **9** (85%), but a poor isolated yield was obtained after purification (36%) due to the presence of many side products.

At this point, the best reaction conditions identified in entry 4 (Table S4†) were used to perform the reaction under μw irradiation in order to decrease the reaction time and side products and improve the efficiency (entry 11). After 2.5 h under μw irradiation, many side products and the significant presence of the C-5 phenyl dihydro TZP derivative **11** were noticed. Thus, the reaction was repeated by adding, after 2 h at 60 °C under μw, H_2O_2 (1 mL) and continuing the reaction in an open flask at 110 °C (entry 12), in order to promote oxidation of **11** to **9**. As expected, the desired oxidation occurred since the peak ratio of compound **9** was 72%, but the reaction showed a lot of side products leading to **9** in a very low yield (12%), after purification by chromatography. Analogously, no interesting results were achieved when performing the reaction in AcOH at 60 °C in the presence of I_2 (entry 13), a catalyst used in the literature to promote cyclocondensation and oxidation in Biginelli MCRs.[26,27]

Thus, the best reaction conditions for the synthesis of compound **11** are reacting **12** (1 equiv.), **13** (1 equiv.), and **14** (1 equiv.) in the presence of citric acid (2.5 equiv.) in EtOH at reflux for 3.5 h (Table 1, entry a). Through this one-step procedure, compound **11** was regioselectively obtained in 83% yield. On the other hand, the best reaction conditions for the synthesis of **9** are reacting **12** (1 equiv.), **13** (3 equiv.) and **14** (1 equiv.) in acetic acid at 60 °C under nitrogen for 9 h (Table 1, entry b). Through this one-step procedure, compound **9** was regioselectively synthesized in 55% yield. Although the procedure for the synthesis of **9** showed a moderate yield, it was more efficient than the two-step procedure entailing the cyclocondensation reaction (83% yield) and the successive oxidation reaction (26% yield), showing a 22% overall yield. To the best of our knowledge, these two procedures are the first Biginelli-like MCRs in which the reaction of an aminotriazole, an aldehyde, and a β-ketoester leads to the formation of ethyl 2-amino-7-methyl-5-phenyl-[1,2,4]triazolo[1,5-*a*]pyrimidine-6-carboxylate compounds.

Focusing our attention on the synthesis of ethyl 2-amino-5-methyl-7-phenyl-[1,2,4]triazolo[1,5-*a*]pyrimidine-6-carboxylate (**8**) and searching for a procedure entailing a single step and without the use of oxidative agents, we evaluated some minor changes in the reaction conditions reported by Chernyshev and co-workers in Scheme 3a. Thus, DMF was first replaced with *N*-methyl-2-pyrrolidone (NMP) or pyridine, but only a complex mixture after 24 h was observed (data not shown). Then, the combination of the use of DMF with 1 equiv. of Et_3N or 1,4-dioxane with 1 equiv. of K_2CO_3 led in both cases to the formation of the azomethine derivative **15** as the main product coupled with an incomplete consumption of the starting material **12** after 24 h (data not shown). The use of additional solvents was strongly affected by the limited solubility of the starting material **12** in most of the common solvents used for chemical reactions. At this point, also considering environmental sustainability, the use of ionic liquids (ILs) as the solvent was studied (Table S5†).

Initially, two ILs, *i.e.*, 1-butyl-3-methylidazolium mesylate (BMIM-MsO) and *N*,*N*,*N*-tributylmethylammonium mesylate (TBMA-MsO)[28] were used with 1 equiv. of each starting material (**12**, **13**, and **14**), and reactions were performed at 120 °C in an open flask up to the disappearance of **12** observed by TLC. Interestingly, on using BMIM-MsO (entry 1), after 48 h, the desired compound **8** was formed in a high percentage as monitored by HPLC (93%). However, after the aqueous reaction work-up and the filtration of the solid, compound **8** was obtained in 30% yield, even if no additional side products or remaining starting material was noticed. On the other hand, the same reaction performed with TBMA-MsO (entry 2) led to the disappearance of **12** after 24 h and the formation of

the non-aromatic isomer **10**, without showing any traces of compound **8**. After the aqueous reaction work-up, compound **10** was obtained as a pure solid in 75% yield (Table 1, entry c). Therefore, the procedure to regioselectively obtain the dihydro-TZP analogue **10** with a high yield through a one-step, three-component reaction and without any purification step was identified.

Since BMIM-MsO allowed us to isolate the aromatic isomer **8** in a modest yield (30%), we considered the use of a similar IL having a different counterion. Thus, the reaction was repeated using the same conditions as entry 1 in BMIM-tetrafluoroborate (BMIM-TFB) (entry 3), but a loss of regioselectivity was observed, thus obtaining compound **8** in 25% yield. At this point, the effect of 2 equiv. of benzaldehyde **13** when using both BMIM-MsO (entry 4) and TBMA-MsO (entry 5) was evaluated. In both cases, after 12 h, **12** disappeared but the azomethine derivative **15** formed as the main product. Based on the observation that oxidation of compound **10** into **8** was accomplished in a low yield (48%, Scheme 3b) and that protection of the amino group led to improved efficiency of the oxidation in analogous TZP compounds,[29] we attempted to oxidize derivative **15** and then deprotect the amino group in the same reaction to achieve compound **8**. Thus, the reaction in three different ILs (entries 6–8) was carried out using 2 equiv. of benzaldehyde **13** and adding a mild and green oxidizing agent such as H_2O_2 (1 mL) after 12 h, at which time the disappearance of diamino-triazole **12** was observed. To our surprise, following the initial formation of the azomethine derivative **15**, we did not observe its oxidation but the formation of the aromatic isomer **8** as the main product in all three reactions was observed. The highest regioselectivity was shown by the reaction performed in BMIM-MsO (entry 6), which, after the aqueous work-up, yielded compound **8** as a pure solid in 40% yield without any purification step (Table 1, entry d). On the other hand, the work-up of the other two reactions (entries 7 and 8) led to very dirty solids.

Based on these results, further studies were undertaken on the role of the equiv. of starting materials in the reaction of entry 6. Thus, the reaction in BMIM-MsO was repeated by using different ratios of the starting materials **12**, **13** and **14** (*i.e.*, 1 : 3 : 1; 1 : 2 : 2; 1 : 1 : 2; 2 : 1 : 1; 2 : 1 : 2) and adding H_2O_2 after the disappearance of the limiting starting material **12**. Although the formation of compound **8** as the main product was observed, several side products characterized these reactions that led to the isolation of non-pure solids (not shown).

Finally, the role of the solvent was investigated by repeating the reaction of entry 6 in other ILs and also in deep eutectic solvents (DESs) (Table S6†). In particular, the reaction of **12** (1 equiv.), **13** (2 equiv.), and **14** (1 equiv.) was performed at 120 °C in six different ILs, *i.e.*, TBMA tosylate (TsO), tributylmethylphosphonium (TBMP) MsO, 1,3-dimethylimidazolium (MMIM) TsO, tetrabutyl ammonium (TBA) TsO, TBA bromide, and TBA-MsO (entries 1–6), and in three different DESs, *i.e.*, ethylene glycol/trimethylglycine (EG/TMG), glycolic acid/trimethylglycine (Gly/TMG), and urea/choline chloride (U/ChCl) (entries 7–9). In all the reactions, H_2O_2 (1 mL) was added after the disappearance of the starting material **12** (6, 20, or 24 h). With the exception of the reaction performed in MMIM-TsO (entry 3), which favoured the formation of compound **15** as the main product, all the other reactions performed in ILs furnished compound **8** as the main product. Nevertheless, all the reactions were characterized by extensive tarring and/or very low efficiency. Analogous results were obtained by the reactions in DESs, which were characterized by the formation of several side products, discouraging the successive work-up. Thus, the best reaction conditions for the synthesis of compound **8** are reacting **12** (1 equiv.), **13** (2 equiv.) and **14** (1 equiv.) in BMIM-MsO at 120 °C for 24 h and adding H_2O_2 (1 mL) after 12 h (Table 1, entry d). Through this one-step procedure, compound **8** was regioselectively obtained in 40% yield. Even though compound **8** was obtained in a moderate yield, this procedure is the first example of the Biginelli MCR in which the reaction between an aminotriazole, an aldehyde and a β-ketoester leads to the formation of an ethyl 2-amino-5-methyl-7-phenyl-[1,2,4]triazolo[1,5-*a*]pyrimidine-6-carboxylate compound. Notably, this one-step MCR procedure having a 40% yield represents to date the best method to obtain oxidized **8**, being more convenient in terms of yield, time, use of a mild oxidizing agent, and a green solvent, with respect to the two-step procedure (formation of **10** and subsequent oxidation, Scheme 3a) exhibiting a 34% overall yield. In addition, by changing some conditions, (*i.e.*, IL, ratio, absence of H_2O_2, and time), for the first time, a novel method to regioselectively obtain the non-aromatic isomer **10** with an improved yield (75% *vs.* 71%) through a one-step MCR, and by using a greener solvent than DMF was also identified (Table 1, entry c).

Plausible pathways accounting for the formation of compounds **10** and **11** through the reaction of **12**, **13**, and **14** are speculatively reported and briefly described in Scheme S1.† In particular, analogously to the three plausible reaction mechanisms proposed for the classic Biginelli reaction,[30] compounds **10** and **11** could be obtained through an imine route (Scheme S1a and d†), an enamine route (Scheme S1b and e†), or a Knoevenagel route (Scheme S1c and f†). While in the imine and enamine routes, the initial reaction plays a key role in the regioselectivity of the reaction, in the Knoevenagel route, the nucleophilic attack of 3,5-diaminotriazole on the adduct is crucial in driving the regioselective formation of **10** or **11**.

Although a deep investigation of the mechanisms involved in this reaction is beyond the scope of this study, the imine and Knoevenagel routes, reported in Scheme 4, were hypothesized to be most likely to occur for the formation of compounds **11** and **10**, respectively. The high rate at which compounds **10** and **11** are formed during the reaction impaired the isolation or TLC monitoring of intermediates. Nevertheless, previous studies provided important information. Indeed, we previously noticed a higher nucleophilicity of the C(3) amino group than the N(2) of **12** under both acidic and basic conditions,[11] advising one to discard the enamine route for the

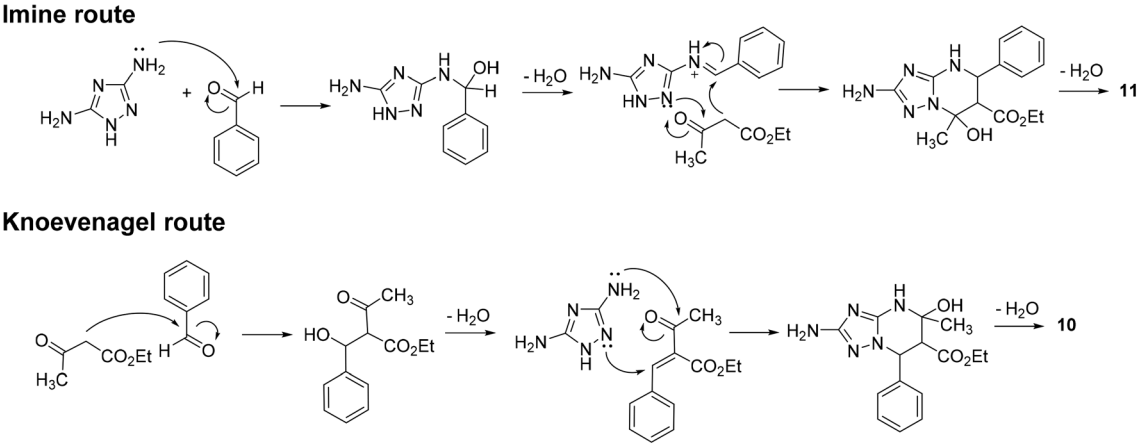

Scheme 4 Plausible reaction mechanisms for the formation of **11** and **10**.

synthesis of **11** (Scheme S1b†) and the imine route for the synthesis of **10** (Scheme S1d†). Regarding compound **11**, we also discarded the Knoevenagel route (Scheme S1c†) based on previous studies suggesting that when reacting with α,β-enone such as Knoevenagel's adduct, the triazole C(3) amino group seems to undergo direct addition at the carbonyl carbon instead of conjugate addition at the β-carbon.[8,11] Thus, in agreement with the most accredited mechanism proposed for the classic Biginelli reaction (which analogously occurs under acidic conditions),[31] the imine route was hypothesized to be most likely to occur for the regioselective synthesis of **11** (Scheme 4).

Focusing on compound **10**, although both the enamine and Knoevenagel routes are possible (Scheme S1e and f†), the latter was the most plausible for us, based on two pieces of information. Firstly, as reported above, the synthesis of compound **10** was reported *via* a two-step procedure involving the initial formation of the Knoevenagel intermediate (Scheme 3b).[24] Secondly, a variation of the classic Biginelli reaction, named Atwal modification,[32,33] envisages the formation of a Knoevenagel intermediate in a neutral or slightly basic environment (analogously to our conditions in the IL) before the addition of urea to form the desired Biginelli compound. To investigate if, analogously, the formation of **10** occurs *via* the Knoevenagel route, we performed two parallel reactions by reacting ethyl 3-oxobutanoate **14** (1 equiv.) with benzaldehyde **13** (1 equiv.) or 3,5-diaminotriazole **12** (1 equiv.) in TBMA-MsO at 110 °C and, after 2 h, we added **12** or **13**, respectively. Only the reaction allowing for the initial generation of Knoevenagel's adduct proceeds towards the formation of **10** after the addition of **12**, thus supporting the hypothesis that the Knoevenagel route could be most likely to occur for the regioselective synthesis of compound **10** (Scheme 4). The regioselectivity of the reaction could be driven, as reported above, by the propensity of the more nucleophilic triazole C(3) amino group to undergo direct addition to the carbonyl carbon of the adduct instead of conjugate addition to the β-carbon.

Synthesis of target compounds 23–30

As mentioned above, for some years, we have been involved in the identification of TZP-based compounds as the inhibitors of RNA viruses, mainly as anti-IV agents by inhibiting the PA–PB1 subunits interaction of viral RdRP. In this study, in order to gain structure–activity relationship insights for this class of compounds, we aimed at studying the role of a substituent at the C-6 position. In particular, to prepare the designed compounds that need to be evaluated for antiviral activity, we exploited scaffolds **8** and **9**, characterized by C-6 ethyl ester, and prepared an additional set of intermediates having carboxamide, *p*-tolyl-carboxamide, and carboxylic acid at the C-6 position.

Firstly, we focused our attention on the synthesis of carboxamide C-6 functionalized scaffolds **16–19** (Schemes 5 and 6) by exploiting the reaction conditions identified for the synthesis of ester derivatives **8** and **9**. Accordingly, the reactions were repeated by replacing ethyl 3-oxobutanoate (**14**) with 3-oxobutanamide (**20**) or *N*-acetoacetyl-*p*-toluidine (**21**). The isomers have been distinguished by NMR based on the chemical shifts of the pyrimidine methyl carbon of aromatic compounds, appearing at 23–24 ppm and 14–16 ppm for the 5-methyl-7-phenyl and 7-methyl-5-phenyl isomers, respectively (Table S1†).

The reaction of **12** (1 equiv.), **13** (3 equiv.), and **20** (1 equiv.) in AcOH at 60 °C furnished compound **16** in 26% yield (Scheme 5). On the other hand, the reaction of **12** (1 equiv.), **13** (2 equiv.), and **20** (1 equiv.) in BMIM-MsO in an open flask at 120 °C with H_2O_2 after the disappearance of **12** furnished compound **17** only in 15% yield (Scheme 5). As an alternative reaction, we attempted to react **12** (1 equiv.), **13** (2 equiv.), and **20** (1 equiv.) in DMF at 130 °C in an open vessel to favour oxidation. Of note, compound **17** was obtained in 42% yield (Scheme 5).

Turning our attention to the synthesis of isomers **18** and **19** (Scheme 6), the reaction of **12**, **13**, and **21** in AcOH at 60 °C for 15 h yielded compound **18** in 25% yield. On the other hand,

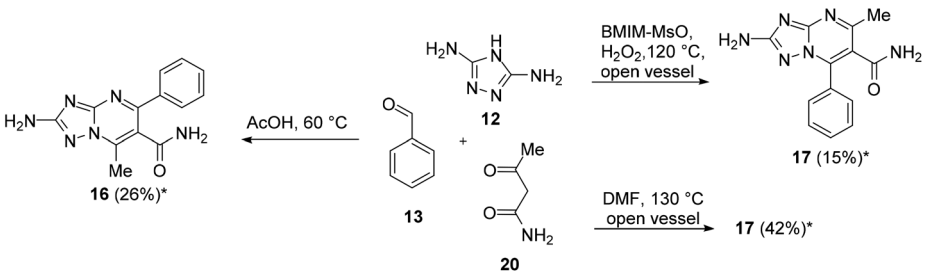

Scheme 5 Chemical procedures for the synthesis of 2-amino-TZP compounds **16** and **17**. *Isolated yield.

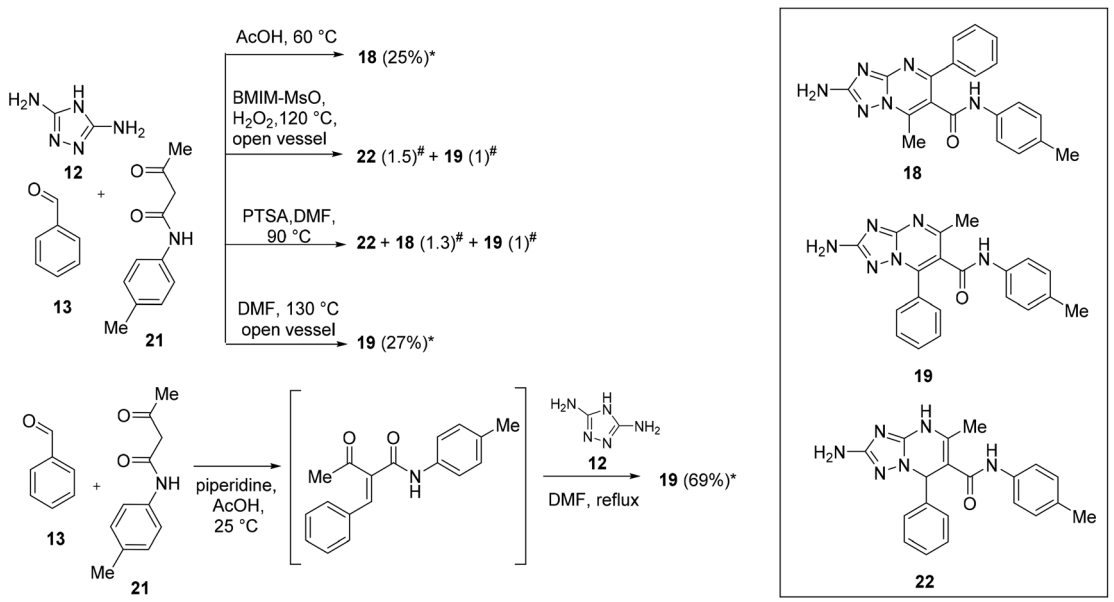

Scheme 6 Chemical procedures for the synthesis of 2-amino-TZP compounds **18** and **19**. *Isolated yield. # Ratios determined by NMR on the crude product.

the reaction in BMIM-MsO furnished a mixture of **19** and non-oxidized analogue **22** in a ratio of 1 : 1.5. Thus, the synthesis of compound **19** was attempted by applying a synthetic procedure reported in the literature, in which the reaction of an equimolar mixture of **12**, **13**, and **21** in DMF in the presence of PTSA (0.05 equiv.) at 90 °C for 16 h furnished the target compound in 58% yield.[34] However, when the reaction was performed under these conditions, a mixture containing several side products was obtained (*i.e.*, the non-oxidized compound **22**, and both the oxidized isomers **18** and **19** in a ratio of 1.3 : 1). Looking at the ^{13}C NMR spectrum reported by the authors for the synthesized compound,[34] the chemical shift of pyrimidine methyl carbon appears at 15.49 ppm, leading to a hypothesis that the compound obtained as the main product by the authors was the 7-methyl-5-phenyl isomer **18** and not the 5-methyl-7-phenyl isomer **19**. Of note, in the manuscript, the authors also reported 22 compounds characterized by different substituents on the C-6 amide moiety, of which the chemical shift of the pyrimidine methyl carbon appears at ~15.5 ppm for 13 compounds and ~23 ppm for 9 compounds, suggesting that the 7-phenyl isomer was not always obtained as the major product as declared by the authors. At this point, the same conditions exploited to obtain compound **17** were used to synthesize compound **19**, which was obtained in a low yield (27%). Thus, we attempted a one-pot two-step reaction entailing the reaction of **13** and **21** in AcOH and piperidine at room temperature followed by the addition of **12** and DMF leading the temperature at reflux. Under these conditions, oxidized compound **19** was directly obtained in 69% yield.

The synthesized scaffolds **8**, **9**, and **16–19** were reacted with benzoyl chloride in pyridine providing target derivatives **23–28** (Scheme 7). Then, to determine the effect of carboxylic acid at the C-6 position of the TZP core, compounds **23** and **26** were hydrolyzed in the presence of LiOH in dioxane, furnishing acid derivatives **29** and **30**, respectively.

The synthesized compounds **23–30** were evaluated for their ability to inhibit the physical interaction between PA and PB1 subunits by an ELISA-based interaction assay (Table 2).

In parallel, for all the synthesized compounds, the anti-IAV activity was tested by plaque reduction assays (PRA) in Madin–

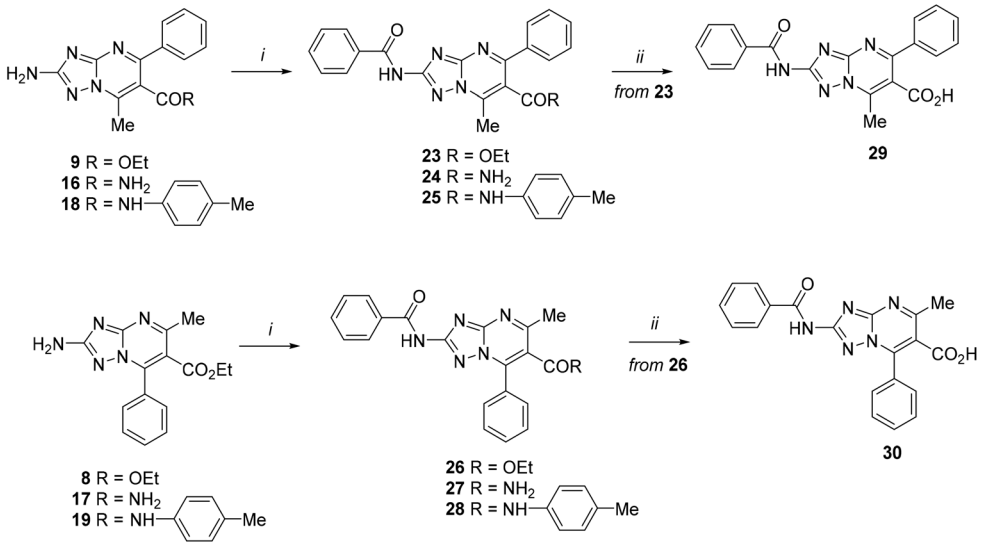

Scheme 7 Reagents and conditions: (i) benzoyl chloride, pyridine, from 0 °C to rt; (ii) LiOH, 1,4-dioxane, 45 or 60 °C.

Table 2 Structures, anti-PA-PB1 and anti-IAV activities, and cytotoxicity of TZPs **23–30** synthesized in this study

Compd	R_6	ELISA PA-PB1 interaction assay IC_{50},[a] μM	PRA in MDCK cells EC_{50},[b] μM	Cytotoxicity (MTT assay) in MDCK cells CC_{50},[c] μM
		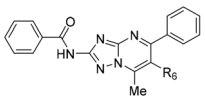		
23	CO_2Et	132 ± 22	>100	>150
29	CO_2H	>200	>100	>250
24	$CONH_2$	109 ± 23	>100	>250
25	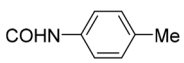	>200	>20	123 ± 74
		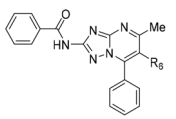		
26	CO_2Et	>200	>100	>250
30	CO_2H	>200	>100	>250
27	$CONH_2$	5.5 ± 1.4	>100	>250
28	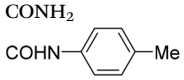	>200	>100	>250
Tat-PB1$_{1-15}$ peptide		35.2 ± 4.7	41.5 ± 5.2	>100
RBV			26.6 ± 5.2	>250

[a] Activity of the compounds in ELISA-based PA–PB1 interaction assays. The IC_{50} value represents the compound concentration that reduces by 50% the interaction between PA and PB1 subunits. [b] Activity of the compounds in plaque reduction assays with the IV A/PR/8/34 strain. The EC_{50} value represents the compound concentration that inhibits 50% of plaque formation. [c] Cytotoxicity of the compounds in MTT assays. The CC_{50} value represents the compound concentration that causes a 50% decrease of cell viability. All the reported values represent the means ± SD of data derived from at least three independent experiments in duplicate. RBV = ribavirin.

Darby canine kidney (MDCK) cells infected with a reference IV, the A/PR/8/34 strain. Ribavirin (RBV), a known broad-spectrum inhibitor of RNA virus polymerases, was also included as a positive control. To exclude that the observed antiviral activities could be due to cytotoxicity on the target cells, the compounds were also tested by MTT assays in MDCK cells.

As shown in Table 2, only compound **27** showed the ability to interfere with the PA–PB1 interaction with an IC_{50} value in the low μM range. However, unfortunately, all the tested compounds were devoid of anti-IV activity. In order to extend the potential antiviral activity of the newly synthesized compounds **23–30**, cell-based antiviral assays were performed against additional RNA viruses, *i.e.*, DENV, WNV, and SARS-CoV-2 (Tables 3 and S7†). Dengue virus (DENV), consisting of 4 serotypes (DENV-1–4), is a mosquito-borne flavivirus and is considered a major public health threat in many countries with

Table 3 Anti-DENV-2, anti-WNV, and anti-SARS-CoV-2 activity, and cytotoxicity of TZP derivatives **25** and **26**

Compd	Anti-DENV-2 activity (Huh7 cells) EC_{50},[a] μM	Anti-WNV activity (Huh7 cells) EC_{50},[a] μM	Cytotoxicity (Huh7 cells) CC_{50},[b] μM	Anti-SARS-CoV-2 activity (A549 cells) EC_{50},[c] μM	Cytotoxicity (A549 cells) CC_{50},[b] μM
25	4.3 ± 1.5	6.7 ± 3.7	18.4 ± 3.5	NA[d]	9.8
26	14.1 ± 4.1	19.3 ± 1.4	141 ± 1	NA	99.9
NRM	—	—	—	0.066 ± 0.007	36
SOF	8.1 ± 1.1	5.3 ± 2.5	>243	>243	>243

[a] Activity of the compounds as determined by the immunodetection assay. The EC_{50} value represents the compound concentration that reduces by 50% the expression of flavivirus envelope proteins in Huh7 cells infected with DENV or WNV. All the reported values represent the means ± SD of data derived from at least two independent experiments in duplicate. [b] Cytotoxicity of the compounds as determined by Cell Titer assay in A549 and Huh cell lines. The CC_{50} value represents the compound concentration that causes a 50% decrease of cell viability. [c] Activity of the compounds as determined by Cell Titer assay. The EC_{50} value represents the compound concentration that reduces by 50% the cytopathic effect in A549 cells infected with SARS-CoV-2. All the reported values represent the means ± SD of data derived from at least two independent experiments in duplicate. [d] NA = not active. NRM = nirmatrelvir, SOF = sofosbuvir.

no approved antiviral therapeutics available.[35] DENV causes about 100–400 million infections each year, and led to 36 100 deaths only in 2019.[36,37] Similar to DENV, WNV is also a zoonotic, mosquito-borne flavivirus, containing a positive-sense, single-stranded RNA genome. Occurring in about 1% of human WNV infections, the neuroinvasive form of the infection represents the most severe form of the disease leading to meningitis, encephalitis, and acute flaccid paralysis/poliomyelitis.[38] Severe acute respiratory syndrome coronavirus 2 (SARS-CoV-2), the causative agent of COVID-19, is an enveloped, positive-sense, single-stranded RNA virus belonging to the genus Betacoronavirus.[39] Although we can consider the pandemic over, SARS-CoV-2 variants may continue to adapt in the human population for years or decades.[40]

The anti-DENV and anti-WNV activities were evaluated by a direct yield reduction assay in Huh7 cells infected with the New Guinea C DENV serotype 2 strain and WNV lineage 1 (Italy/2009) strain, respectively. Sofosbuvir (SOF) was used as a reference compound. Anti-SARS-CoV-2 activity was evaluated by a direct yield reduction assay in A549 cells infected with the SARS-CoV-2 strain belonging to lineage B.1. Nirmatrelvir (NRM) was used as a reference compound. In parallel, the cytotoxicity of compounds was determined by CellTiter-Glo 2.0 Luminescent Cell Viability Assay in Huh7 and A549 cells.

As shown in Table S7,† all the compounds were devoid of anti-SARS-CoV-2 activity and most of the compounds did not show anti-flavivirus activity. On the other hand, compounds **25** and **26** stood out as anti-flavivirus agents (Table 3). In particular, compound **25** showed EC_{50} values of 4.3 and 6.7 μM against DENV-2 and WNV, respectively, albeit it also showed certain cytotoxicity (CC_{50} = 18.4 μM). Instead, with EC_{50} values of 14.1 and 19.3 μM against DENV-2 and WNV, respectively, compound **26** was slightly less active but also markedly less toxic (CC_{50} = 141.1 μM), thus showing a promising selectivity index.

Conclusions

In this work, four facile one-step Biginelli-like MCRs for the regioselective synthesis of ethyl 2-amino-[1,2,4]triazolo[1,5-*a*]pyrimidine-6-carboxylates were developed. The regioselectivity of the procedures was achieved by switching from an acidic environment, which allowed us to obtain ethyl 2-amino-7-methyl-5-phenyl-TZP-6-carboxylate **9** and its 4,7-dihydro analogue **11**, to the use of ILs as a solvent, which resulted in ethyl 2-amino-5-methyl-7-phenyl-TZP-6-carboxylate **8** and its 4,7-dihydro analogue **10**. In particular, aromatic derivative **9** was obtained in 55% yield by using AcOH as a solvent, while dihydro-TZP derivative **11** was synthesized in 83% yield under mild acidic conditions with citric acid in EtOH. On the other hand, different ILs were used to selectively obtain compound **10** in 75% yield and aromatic analogue **8** in 40% yield, with the *in situ* oxidation reaction prompted by performing the reaction in an open flask and adding H_2O_2.

Although the two aromatic isomers **8** and **9** were not obtained in high yields, the two procedures represent the first examples of Biginelli-like MCRs in which aromatic TZP compounds have been regioselectively obtained; moreover, they were more efficient than the two-step procedure entailing the cyclocondensation reaction and the successive oxidation reaction.

The reaction in AcOH was also suitable to obtain aromatic 2-amino-7-methyl-5-phenyl-TZPs modified at the C-6 position, although not efficiently (about 25% yield). On the other hand, the reaction in the IL was not suitable to obtain C-6-modified aromatic 2-amino-5-methyl-7-phenyl-TZPs, which however, were obtained through two different chemical procedures in 42% and 69% yields.

In conclusion, it was evident that the electronic properties of the C-6 substituent strongly affect the reactivity of the reagent with an active methylene group needed to carry out the Biginelli-like MCR. Therefore, further efforts should be directed to the identification of reaction conditions compatible with the use of reactants as different as possible in order to extend the use of this MCR for the synthesis of several variously functionalized TZP compounds.

Regarding the biological activity of the new TZP-based compounds reported in this article, antiviral activities were evaluated against RNA viruses, *i.e.*, IV, DENV-2, WNV, and SARS-CoV-2. Compounds **25** and **26** showed the ability to inhibit the viral replication of DENV-2 and WNV at concen-

trations in the low micromolar range, suggesting the use of the TZP scaffold in the discovery of anti-flavivirus agents. Indeed, these results are of particular interest since these compounds are the first TZP-based derivatives showing anti-flavivirus activity, thus paving the way for the design of new analogues.

Experimental

General chemistry

Commercially available starting materials, reagents, and solvents were used as supplied. All reactions were routinely monitored by TLC on silica gel 60F254 (Merck) and visualized using UV or iodine. Flash column chromatography was performed on Merck silica gel 60 (mesh 230–400). After extraction, organic solutions were dried over anhydrous Na_2SO_4, filtered, and concentrated with a Büchi rotary evaporator at reduced pressure. Melting points were determined in capillary tubes (Stuart SMP30) and were uncorrected. Yields are of purified products and were not optimized. ^{1}H NMR and ^{13}C NMR spectra were recorded on Bruker Avance DRX-400. Chemical shifts (δ) are reported in ppm relative to TMS and calibrated using residual undeuterated solvent as the internal reference. Coupling constants (J) are reported in Hz. The spectra were acquired at 298 K. Data processing was performed with Bruker TopSpin 4.2.0 software, and the spectral data are consistent with the assigned structures. The spin multiplicities are indicated using the symbols: s (singlet), d (doublet), t (triplet), q (quartet), m (multiplet), and bs (broad singlet). FT-IR measurements were carried out using a Shimadzu IR-8000 spectrophotometer (Kyoto, Japan). The spectral range measured was from 400 to 4000 cm^{-1}, with a spectral resolution of 4 cm^{-1} acquiring 50 scans. The purity (>95%) of compounds was revealed at 254 nm and λ_{max} of each compound by HPLC analysis using a Jasco LC-4000 instrument equipped with a UV-Visible Diode Array Jasco MD-4015 and an XTerra MS C18 Column, 5 μm, 4.6 mm × 150 mm. The methods and columns used have been specified for each compound. Chromatograms were analyzed using ChromNAV 2.0 Chromatography Data System software and the peak retention time is given in minutes. HRMS spectra were registered on an Agilent 6560 Ion Mobility Q-TOF LC/MS system.

Ethyl 2-amino-5-methyl-7-phenyl-[1,2,4]triazolo[1,5-*a*] pyrimidine-6-carboxylate (8)

Method 1. AcONa (0.041 g, 0.50 mmol) was added to a suspension of **10** (0.1 g, 0.33 mmol) in EtOH (3 mL) and the reaction mixture was heated at 40 °C for 15 min. Then, NBS (0.176 g, 0.99 mmol) was added, and the reaction was refluxed for 24 h. After cooling, the reaction mixture was poured into a saturated solution of $NaHCO_3$ in water, obtaining a precipitate that was filtered and extracted in water at pH 8–9 to give **8** (0.047 g, 48%).

Method 2. BMIM-MsO was heated at 120 °C and, then, **12** (0.20 g, 2.02 mmol), **13** (0.41 mL, 4.04 mmol), and **14** (0.26 mL, 2.02 mmol) were added to an open flask. After 3 h, H_2O_2 (1 mL) was added and the reaction mixture was maintained at 120 °C for 21 h. Then, it was poured into ice/water obtaining a precipitate that was filtered to give **8** as a white solid (0.24 g, 40%); m. p. = 225.3–226.0 °C. ^{1}H NMR (400 MHz, DMSO-d_6) δ: 0.84 (t, J = 7.1 Hz, 3H, OCH_2CH_3), 2.57 (s, 3H, CH_3), 4.00 (q, J = 7.1 Hz, 2H, OCH_2CH_3), 6.51 (bs, 2H, NH_2), 7.56 (m, 5H, Ar–H). ^{13}C NMR (101 MHz, DMSO-d_6) δ: 13.79, 23.93, 61.91, 114.69, 128.87, 129.40, 130.54, 130.91, 144.63, 155.04, 159.56, 166.09, 168.56. FT-IR: 3463.70, 3286.52, 3206.50, 2986.44, 2933.57, 1713.27, 764.47 cm^{-1}. HRMS (ESI) m/z $[M + H]^+$ calcd for $C_{15}H_{15}N_5O_2$ 298.1299 found 298.1311.

Ethyl 2-amino-7-methyl-5-phenyl-[1,2,4]triazolo[1,5-*a*] pyrimidine-6-carboxylate (9)

Method 1. AcONa (0.08 g, 0.96 mmol) was added to a suspension of **11** (0.14 g, 0.48 mmol) in EtOH (3 mL) and the reaction mixture was heated at 40 °C for 15 min. Then, NBS (0.13 g, 0.72 mmol) was added and the reaction was refluxed for 3 h. After cooling, the reaction mixture was poured into a saturated solution of $NaHCO_3$ in water, obtaining a precipitate that was filtered and purified by flash column chromatography eluted with $CHCl_3$/MeOH (97 : 3) to give **9** (0.04 g, 26%).

Method 2. Compounds **13** (0.62 mL, 6.06 mmol) and **14** (0.26 mL, 2.02 mmol) were added to a suspension of **12** (0.2 g, 2.02 mmol) in AcOH (6 mL) under nitrogen and the reaction mixture was maintained at 60 °C for 9 h. Then, it was poured into a saturated solution of $NaHCO_3$ in water, obtaining a precipitate that was filtered and purified by Reveleris-X2 eluted with $CHCl_3$ 100% for 10 min and $CHCl_3$/MeOH (90 : 10 for 10 min) to give **9** as a white solid (0.33 g, 55%); m. p. = 211.8–212.6 °C.^{1}H NMR (400 MHz, DMSO-d_6) δ: 0.93 (t, J = 7.1 Hz, 3H, OCH_2CH_3), 2.73 (s, 3H, CH_3), 4.09 (q, J = 7.1 Hz, 2H, OCH_2CH_3), 6.65 (bs, 2H, NH_2), 7.42–7.64 (m, 5H, Ar–H). ^{13}C NMR (101 MHz, DMSO-d_6) δ: 13.84, 15.79, 62.20, 113.93, 128.44, 128.96, 130.04, 139.16, 145.51, 154.45, 158.67, 166.52, 168.71. FT-IR: 3382.25, 3309.38, 3175.06, 2983.58, 2937.86, 1713.27, 767.33 cm^{-1}. HRMS (ESI) m/z $[M + H]^+$ calcd for $C_{15}H_{15}N_5O_2$ 298.1299 found 298.1315.

Ethyl 2-amino-5-methyl-7-phenyl-4,7-dihydro-[1,2,4]triazolo [1,5-*a*]pyrimidine-6 carboxylate (10)[24]

TBMA-MsO was heated at 120 °C and then, **12** (0.20 g, 2.02 mmol), **13** (0.20 mL, 2.02 mmol), and **14** (0.26 mL, 2.02 mmol) were added to an open flask. After 24 h, the reaction mixture was poured into ice/water obtaining a precipitate that was filtered to give **10** as a pale-yellow solid (0.45 g, 75%); m. p. = 230.2–231.0 °C. ^{1}H NMR (400 MHz, DMSO-d_6): δ 1.02 (t, J = 7.1 Hz, 3H, OCH_2CH_3), 2.37 (s, 3H, CH_3), 3.89–3.96 (m, 2H, OCH_2CH_3), 5.20 (s, 2H, NH_2), 5.94 (s, 1H, H-7), 7.15–7.18 (m, 2H, Ar–H), 7.21–7.25 (m, 1H, Ar–H), 7.26–7.31 (m, 2H, Ar–H), 10.47 (s, 1H, NH). ^{13}C NMR (101 MHz, DMSO-d_6): δ 14.46, 18.98, 59.32, 59.73, 97.74, 127.53, 128.12, 128.71, 143.25, 146.28, 146.97, 162.68, 165.87. FT-IR: 3470.85, 3297.95, 3192.21, 2976.44, 2933.57, 1697.56, 750.18 cm^{-1}. HRMS (ESI) m/z $[M + H]^+$ calcd for $C_{15}H_{17}N_5O_2$ 300.1455 found 300.1469.

Ethyl 2-amino-7-methyl-5-phenyl-4,7-dihydro-[1,2,4]triazolo [1,5-*a*]pyrimidine-6 carboxylate (11)

Compounds **13** (0.21 mL, 2.02 mmol) and **14** (0.26 mL, 2.02 mmol), and citric acid (0.97 g, 5.05 mmol) were added to a suspension of **12** (0.2 g, 2.02 mmol) in EtOH (6 mL) under nitrogen and the reaction mixture was refluxed for 3.5 h. Then, it was poured into ice/water obtaining a precipitate that was filtered to give **11** as a yellow solid (0.50 g, 83%); m. p. = 218.4–218.9 °C. ^{1}H NMR (400 MHz, DMSO-d_6) δ: 1.17 (t, J = 7.1 Hz, 3H, OCH$_2$*CH*$_3$), 2.56 (s, 3H, CH$_3$), 4.09 (q, J = 7.1 Hz, 2H, O*CH*$_2$CH$_3$), 5.46 (d, J = 3.2 Hz, 1H, H-7), 5.62 (s, 2H, NH$_2$), 7.21–7.25 (m, 2H, Ar–H), 7.25–7.30 (m, 1H, Ar–H), 7.32–7.34 (m, 2H, Ar–H), 8.55 (d, J = 3.2 Hz, 1H, NH). ^{13}C NMR (101 MHz, DMSO-d_6) δ: 14.64, 15.73, 53.15, 60.40, 101.12, 126.37, 128.18, 129.13, 143.80, 144.88, 154.11, 164.09, 165.92. FT-IR: 3420.83, 3312.24, 3179.35, 2979.30, 1683.27, 1633.26, 755.90 cm^{-1}. HRMS (ESI) m/z [M + H]$^+$ calcd for $C_{15}H_{17}N_5O_2$ 300.1455 found 300.1458.

2-Amino-7-methyl-5-phenyl-[1,2,4]triazolo[1,5-*a*]pyrimidine-6-carboxamide (16)

The title compound was synthesized by following the same procedure as that used for the synthesis of **9** (method 2, 3 h) in 26% yield. ^{1}H NMR (400 MHz, DMSO-d_6) δ: 2.66 (s, 3H, CH$_3$), 6.57 (s, 2H, NH$_2$), 7.45–7.51 (m, 3H, Ar–H), 7.75–7.80 (m, 3H, CONH$_2$ and Ar–H), 7.98 (s, 1H, CONH$_2$). ^{13}C NMR (101 MHz, DMSO-d_6) δ: 14.47, 117.78, 127.55, 127.81, 128.84, 137.63, 142.02, 153.07, 155.73, 166.52, 167.29. HRMS (ESI) m/z [M + H]$^+$ calcd for $C_{13}H_{12}N_6O$ 269.1146 found 269.1159.

2-Amino-5-methyl-7-phenyl-[1,2,4]triazolo[1,5-*a*]pyrimidine-6-carboxamide (17)

A mixture of **12** (0.2 g, 2.02 mmol), **13** (0.20 mL, 2.02 mmol), and **20** (0.20 g, 2.02 mmol) in DMF (6 mL) was heated at 130 °C for 2 h in an open flask. After cooling, the reaction mixture was poured into ice/water and filtered to give **17** as a pale-yellow solid (0.23 g, 42%). ^{1}H NMR (400 MHz, DMSO-d_6) δ: 2.54 (s, 3H, CH$_3$), 6.38 (s, 2H, NH$_2$), 7.49–7.70 (m, 6H, Ar–H and CONH), 7.84 (s, 1H, CONH). ^{13}C NMR (101 MHz, DMSO-d_6): δ 23.24, 119.80, 128.66, 129.89, 130.05, 130.82, 142.24, 154.69, 158.87, 167.16, 167.99. HRMS (ESI) m/z [M + H]$^+$ calcd for $C_{13}H_{12}N_6O$ 269.1803 found 269.1160.

2-Amino-7-methyl-5-phenyl-*N*-(*p*-tolyl)-[1,2,4]triazolo[1,5-*a*] pyrimidine-6-carboxamide (18)

The title compound was synthesized by following the same procedure as that used for the synthesis of **9** (method 2, 15 h). After purification by flash chromatography (Reveleris-X2) eluted with CHCl$_3$/MeOH (from 99 : 1 to 97 : 3), compound **18** was obtained as a yellow solid in 25% yield. ^{1}H NMR (400 MHz, DMSO-d_6) δ: 2.24 (s, 3H, tolyl-CH$_3$), 2.69 (s, 3H, CH$_3$), 6.63 (s, 2H, NH$_2$), 7.10 and 7.35 (d, J = 8.4 Hz, each 2H, Ar–H), 7.40–7.50 (m, 3H, Ar–H), 7.72–7.82 (m, 2H, Ar–H), 10.40 (s, 1H, NH). ^{13}C NMR (101 MHz, DMSO-d_6) δ: 15.68, 21.03, 118.61, 120.22, 128.83, 129.74, 130.13, 133.81, 136.42, 138.57, 143.86, 154.41, 157.24, 164.01, 168.61. HRMS (ESI) m/z [M + H]$^+$ calcd for $C_{20}H_{18}N_6O$ 359.1615 found 359.1629.

2-Amino-5-methyl-7-phenyl-*N*-(*p*-tolyl)-[1,2,4]triazolo[1,5-*a*] pyrimidine-6-carboxamide (19)

A mixture of **13** (0.23 mL, 2.22 mmol), **21** (0.39 g, 2.02 mmol), and piperidine (0.1 mL, 1.01 mmol) in AcOH (0.06 mL, 1.01 mmol) was stirred at 25 °C for 2 h. Then, **12** (0.2 g, 2.02 mmol) and DMF (2 mL) were added and the reaction was stirred at reflux for 14 h. The mixture was poured into ice/water to give a precipitate that was filtered and purified by flash chromatography eluted with CHCl$_3$/MeOH (95 : 5), furnishing **19** as a yellow solid (0.5 g, 69%). ^{1}H NMR (400 MHz, DMSO-d_6) δ: 2.22 (s, 3H, tolyl-CH$_3$), 2.57 (s, 3H, CH$_3$), 6.47 (s, 2H, NH$_2$), 7.07 and 7.27 (d, J = 7.9 Hz, each 2H, Ar–H), 7.47–7.53 (m, 3H, Ar–H), 7.66–7.72 (m, 2H, Ar–H), 10.31 (s, 1H, NH). ^{13}C NMR (101 MHz, DMSO-d_6) δ: 21.00, 23.24, 119.41, 120.10, 128.74, 129.69, 129.74, 129.82, 130.99, 133.77, 136.31, 142.90, 154.90, 159.13, 163.53, 168.24. HRMS (ESI) m/z [M + H]$^+$ calcd for $C_{20}H_{18}N_6O$ 359.1615 found 359.1627.

General procedure for C-2 amidation (Method A)

Benzoyl chloride (1.2 equiv.) was added dropwise at 0 °C to a solution of 2-amino-[1,2,4]triazolo[1,5-*a*]pyrimidine **8**, **9**, or **16–19** (1.0 equiv.) in dry pyridine and the reaction mixture was maintained at rt until the starting material was not detected by TLC (80 min–2 h). Then, the reaction mixture was poured into ice/water and 2 N HCl was added (pH ~ 5–7), obtaining a precipitate that was filtered and purified as described.

Ethyl 2-benzamido-7-methyl-5-phenyl-[1,2,4]triazolo[1,5-*a*] pyrimidine-6-carboxylate (23)

The title compound was synthesized starting from compound **9** by Method A (80 min) and purified by flash chromatography eluted with CHCl$_3$/MeOH (99 : 1) as a white solid in 60% yield; m. p. = 238.2–239.0 °C. ^{1}H NMR (400 MHz, DMSO-d_6) δ: 0.95 (t, J = 6.9 Hz, 3H, OCH$_2$*CH*$_3$), 2.88 (s, 3H, CH$_3$), 4.14 (q, J = 6.9 Hz, 2H, O*CH*$_2$CH$_3$), 7.52–7.59 (m, 5H, Ar–H), 7.61–7.63 (m, 3H, Ar–H), 8.05 (d, J = 7.6 Hz, 2H, Ar–H), 11.57 (s, 1H, CONH). ^{13}C NMR (101 MHz, DMSO-d_6) δ: 13.86, 15.96, 62.58, 116.04, 128.57, 128.72, 192.02, 129.16, 130.56, 132.83, 134.08, 138.68, 148.17, 153.40, 160.84, 161.89, 165.35, 166.10. HPLC, 0.7 mL min^{-1}, H$_2$O 40%/CH$_3$CN 60%, ret. time: 3.2133 min. HRMS (ESI) m/z [M + H]$^+$ calcd for $C_{22}H_{19}N_5O_3$ 402.1561 found 402.15619.

2-Benzamido-7-methyl-5-phenyl-[1,2,4]triazolo[1,5-*a*] pyrimidine-6-carboxamide (24)

The title compound was synthesized starting from compound **16** by Method A (1 h) and purified by crystallization by a mixture of EtOH/DMF as a white solid in 64% yield; m. p. = 284.6–286.0 °C. ^{1}H NMR (400 MHz, DMSO-d_6) δ: 2.82 (s, 3H, CH$_3$), 7.51–7.58 (m, 5H, Ar–H), 7.61–76.3 (m, 1H, Ar–H), 7.83–7.91 (m, 3H, Ar–H and CONH$_2$), 8.04–8.09 (m, 3H, Ar–H and CONH$_2$), 11.49 (s, 1H, CONH). ^{13}C NMR (101 MHz, DMSO-d_6) δ: 15.77, 120.90, 128.69, 128.89, 129.03, 129.12, 130.56,

132.80, 134.09, 138.35, 145.55, 153.17, 159.64, 161.54, 165.44, 167.14. HPLC, 0.5 mL min^{-1}, H_2O (0.1% FA) 80%/CH_3CN 20% to CH_3CN 100% in 10 min, ret. time: 6.8367 min. HRMS (ESI) m/z $[M + H]^+$ calcd for $C_{20}H_{16}N_6O_2$ 373.1408 found 373.14145.

2-Benzamido-7-methyl-5-phenyl-*N*-(*p*-tolyl)-[1,2,4]triazolo[1,5-*a*]pyrimidine-6-carboxamide (25)

The title compound was synthesized starting from **18** by Method A (80 min) and purified by flash chromatography eluted with $CHCl_3$/MeOH (99 : 1) as a pale pink solid in 55% yield; m. p. = 255.3–256.9 °C. ^{1}H NMR (400 MHz, DMSO-d_6) δ: 2.25 (s, 3H, tolyl-CH_3), 2.86 (s, 3H, CH_3), 7.12 and 7.36 (d, J = 8.0 Hz, each 2H, Ar–H), 7.45–7.51 (m, 3H, Ar–H), 7.55 (t, J = 7.4 Hz, 2H, Ar–H), and 7.64 (t, J = 7.4 Hz, 1H, Ar–H), 7.79–7.87 (m, 2H, Ar–H), 8.06 (d, J = 8.1 Hz, 2H, Ar–H), 10.51 and 11.54 (s, each 1H, CONH). ^{13}C NMR (101 MHz, DMSO-d_6) δ: 15.80, 21.04, 120.32, 120.49, 128.71, 129.00, 129.04, 129.81, 130.68, 132.83, 134.07, 136.21, 138.13, 146.35, 153.34, 159.93, 161.77, 163.43, 165.45. HPLC, 0.6 mL min^{-1}, H_2O (0.1% FA) 50%/CH_3CN 50% to CH_3CN 100% in 10 min, ret. time: 5.7000 min. HRMS (ESI) m/z $[M + H]^+$ calcd for $C_{27}H_{22}N_6O_2$ 463.1877 found 463.18877.

Ethyl 2-benzamido-5-methyl-7-phenyl-[1,2,4]triazolo[1,5-*a*]pyrimidine-6-carboxylate (26)

The title compound was synthesized starting from compound **8** by Method A (2 h) and purified by flash chromatography eluted with $CHCl_3$/MeOH (98 : 2) as a white/yellowish solid in 86% yield; m. p. = 250.1–251.7 °C. ^{1}H NMR (400 MHz, DMSO-d_6) δ: 0.88 (t, J = 7.0 Hz, 3H, OCH_2CH_3), 2.68 (s, 3H, CH_3), 4.07 (q, J = 7.1 Hz, 2H, OCH_2CH_3), 7.46–7.55 (m, 2H, Ar–H), 7.57–7.70 (m, 6H, Ar–H), 7.98 (d, J = 7.7 Hz, 2H, Ar–H), 11.42 (s, 1H, CONH). ^{13}C NMR (101 MHz, DMSO-d_6) δ: 13.84, 24.23, 62.34, 117.16, 128.66, 128.97, 129.04, 129.70, 131.47, 132.77, 133.98, 146.44, 154.09, 161.64, 161.91, 165.29, 165.71. HPLC, 0.7 mL min^{-1}, H_2O 40%/CH_3CN 60%, ret. time: 3.0100 min. HRMS (ESI) m/z $[M + H]^+$ calcd for $C_{22}H_{19}N_5O_3$ 402.1561 found 402.15669.

2-Benzamido-5-methyl-7-phenyl-[1,2,4]triazolo[1,5-*a*]pyrimidine-6-carboxamide (27)

The title compound was synthesized starting from compound **17** by Method A (1 h) and purified by flash chromatography eluted with $CHCl_3$/MeOH (97 : 3) as a brown solid in 81% yield; m. p. = 248.2–248.9 °C. ^{1}H NMR (400 MHz, DMSO-d_6) δ: 2.66 (s, 3H, CH_3), 7.50 (t, J = 7.3 Hz, 2H, Ar–H), 7.56–7.64 (m, 4H, Ar–H), 7.72–7.79 (m, 3H, $CONH_2$ and Ar–H), 7.94–7.98 (m, 3H, $CONH_2$ and Ar–H), 11.33 (s, 1H, CONH). ^{13}C NMR (101 MHz, DMSO-d_6) δ: 23.63, 121.94, 128.62, 128.82, 128.97, 129.30, 130.13, 131.33, 132.73, 134.00, 143.85, 153.76, 160.98, 161.93, 165.43, 166.62. HPLC, 0.5 mL min^{-1}, H_2O (0.1% FA) 80%/CH_3CN 20% to CH_3CN 100% in 10 min, ret. time: 5.5500 min. HRMS (ESI) m/z $[M + H]^+$ calcd for $C_{20}H_{16}N_6O_2$ 373.1408 found 373.14107.

2-Benzamido-5-methyl-7-phenyl-*N*-(*p*-tolyl)-[1,2,4]triazolo[1,5-*a*]pyrimidine-6-carboxamide (28)

The title compound was synthesized starting from **19** by Method A (1 h) and purified by crystallization by a mixture of EtOH/DMF as a white solid in 70% yield; m. p. = 240.3–240.9 °C. ^{1}H NMR (400 MHz, DMSO-d_6) δ: 2.23 (s, 3H, tolyl-CH_3), 2.69 (s, 3H, CH_3), 7.09 and 7.28 (d, J = 7.9 Hz, 2H, Ar–H), 7.47–7.58 (m, 5H, Ar–H), 7.59–7.63 (m, 1H, Ar–H), 7.72–7.81 (m, 2H, Ar–H), 7.99 (d, J = 7.4 Hz, 2H, Ar–H), 10.39 and 10.41 (s, each 1H, CONH).^{13}C NMR (101 MHz, DMSO-d_6) δ: 21.02, 23.64, 120.24, 121.48, 128.64, 128.90, 128.99, 129.09, 129.77, 129.99, 131.51, 132.76, 134.00, 136.10, 144.66, 153.94, 161.27, 162.12, 162.97, 165.43. HPLC, 0.5 mL min^{-1}, H_2O (0.1% FA) 35%/CH_3CN 65%, ret. time: 4.3967 min. HRMS (ESI) m/z $[M + H]^+$ calcd for $C_{27}H_{22}N_6O_2$ 463.1877 found 463.18948.

2-Benzamido-7-methyl-5-phenyl-[1,2,4]triazolo[1,5-*a*]pyrimidine-6-carboxylic acid (29)

1M solution of LiOH in H_2O (16.80 mL, 16.80 mmol) was added to a solution of **23** (0.65 g, 1.68 mmol) in 1,4-dioxane (18 mL), and the reaction mixture was stirred at 60 °C for 24 h. Then, the reaction mixture was poured into ice/water and HCl was added until pH ≈ 3, obtaining a precipitate that was filtered. After purification by flash chromatography elution with $CHCl_3$/MeOH (95 : 5), **29** was obtained as a white solid (0.207 g, 74%); m. p. > 300 °C. ^{1}H NMR (400 MHz, DMSO-d_6) δ: 2.50 (s, 3H, CH_3), 7.36–7.42 (m, 5H, Ar–H), 7.50 (t, J = 7.1 Hz, 2H, Ar–H), 7.62 (t, J = 7.0 Hz, 1H, Ar–H), 7.98 (d, J = 7.2 Hz, 2H, Ar–H), 11.73 (bs, 1H, CONH). ^{13}C NMR (101 MHz, DMSO) δ: 32.70, 110.53, 128.26, 128.56, 128.68, 128.95, 129.08, 133.17, 133.31, 141.93, 155.44, 157.33, 157.52, 164.67, 166.30, 200.24. HPLC, 0.8 mL min^{-1}, MeOH (0.1% FA) 30%/H_2O (0.1% FA) 30%/CH_3CN (0.1% FA) 40%, ret. time: 2.3500 min. HRMS (ESI) m/z $[M + H]^+$ calcd for $C_{20}H_{15}N_5O_3$ 374.1248 found 374.12503.

2-Benzamido-5-methyl-7-phenyl-[1,2,4]triazolo[1,5-*a*]pyrimidine-6-carboxylic acid (30)

The title compound was synthesized starting from **26** using the same synthetic procedure as that used for compound **29** (45 °C for 1 h), and purified by crystallization using a mixture of EtOH/DMF in 78% yield; m. p. > 300 °C. ^{1}H NMR (400 MHz, DMSO-d_6) δ: 2.26 (s, 3H, CH_3), 7.48–7.58 (m, 4H, Ar–H), 7.59–7.70 (m, 2H, Ar–H), 7.90–7.97 (m, 2H, Ar–H), 7.98–8.05 (m, 2H, Ar–H), 11.30 (s, 1H, CONH), 13.71 (bs, 1H, COOH). ^{13}C NMR (101 MHz, DMSO-d_6) δ: 18.05, 111.28, 128.64, 129.03, 129.28, 129.87, 132.78, 134.08, 134.28, 137.94, 150.00, 151.20, 154.66, 157.73, 165.45, 193.72. HPLC, 0.5 mL min^{-1}, H_2O (0.1% FA) 65%/CH_3CN (0.1% FA) 35% to CH_3CN (0.1% FA) 100% in 12 min, ret. time: 6.9467 min. HRMS (ESI) m/z $[M + H]^+$ calcd for $C_{20}H_{15}N_5O_3$ 374.1248 found 374.12512.

Biological evaluation (IV)

Compounds and the peptide. RBV (1-D-ribofuranosyl-1,2,4-triazole-3-carboxamide) was purchased from Roche. Each test compound was dissolved in 100% DMSO. The $PB1_{(1–15)}$-Tat

peptide was synthesized and purified by the Peptide Facility of CRIBI Biotechnology Center (University of Padua, Padua, Italy). This peptide corresponds to the first 15 amino acids of the PB1 protein fused to a short sequence of the HIV Tat protein (amino acids 47–59), which allows their delivery into the cell.[41]

Cells and virus. Madin-Darby canine kidney (MDCK) and human embryonic kidney (HEK) 293T cells were grown in Dulbecco's modified Eagle's medium (DMEM, Life Technologies) supplemented with 10% (v/v) fetal bovine serum (FBS, Life Technologies) and antibiotics (100 U mL^{-1} penicillin and 100 μg mL^{-1} streptomycin, Life Technologies). The cells were maintained at 37 °C under a humidified atmosphere with 5% CO_2. The IVA/PR/8/34 strain (H1N1, Cambridge lineage) was kindly provided by P. Digard (Roslin Institute, University of Edinburgh, United Kingdom).

PA–PB1 interaction enzyme-linked immunosorbent assay (ELISA). The PA–PB1 interaction was detected using a previously described procedure.[42,43] Briefly, 96-well microtiter plates (Nuova Aptaca) were coated with 400 ng of 6His-$PA_{(239–716)}$ for 3 h at 37 °C and then blocked with 2% BSA (Sigma) in PBS for 1 h at 37 °C. The 6His-$PA_{(239–716)}$ protein was expressed in *E. coli* strain BL21(DE3)pLysS and purified as already described.[42] After washing, 200 ng of GST-$PB1_{(1–25)}$, or GST alone as a control, in the absence or the presence of test compounds at various concentrations, were added and incubated O/N at room temperature. *Escherichia coli*-expressed, purified GST and GST-$PB1_{(1–25)}$ proteins were obtained as previously described.[42,44] After washing, the interaction between 6His-$PA_{(239–716)}$ and GST-$PB1_{(1–25)}$ was detected with a horseradish peroxidase-coupled anti-GST monoclonal antibody (GenScript) diluted 1 : 4000 in PBS supplemented with 2% FBS. Following the washings, substrate 3,3′,5,5′-tetramethylbenzidine (TMB, KPL) was added and the absorbance was measured at 450 nm using an ELISA plate reader (MultiSkan FC, Thermo Scientific). The values obtained from the samples treated with only DMSO were used to set 100% of PA–PB1 interaction.

Cytotoxicity assay. The cytotoxicity of compounds was tested in MDCK cells using the 3-(4,5-dimethylthiazol-2-yl)-2,5-diphenyl tetrazolium bromide (MTT) method, as previously reported.[42,45] Briefly, MDCK cells (seeded at a density of 2×10^4 per well) were grown in 96-well plates for 24 h and then treated with serial dilutions of test compounds, or DMSO as a control, in DMEM supplemented with 10% FBS. After incubation at 37 °C for 48 h, 5 mg mL^{-1} of MTT (Sigma) in PBS was added into each well and incubated at 37 °C for a further 4 h. Successively, a solubilized solution was added to lyse the cells and incubated O/N at 37 °C. Finally, optical density was read at a wavelength of 620 nm on a microtiter plate reader (MultiSkan FC, Thermo Scientific).

Plaque reduction assay (PRA). The antiviral activity of test compounds against IVA was tested by PRA as previously described.[46] MDCK cells were seeded at 5×10^5 cells per well into 12-well plates and incubated at 37 °C for 24 h. On the following day, the culture medium was removed and the monolayers were first washed with serum-free DMEM and then infected with the IVA/PR/8/34 strain at 40 PFU per well in DMEM supplemented with 1 μg mL^{-1} of TPCK-treated trypsin (Worthington Biochemical Corporation) and 0.14% BSA and incubated for 1 h at 37 °C. The IV infection was performed in the presence of different concentrations of test compounds or solvent (DMSO) as a control. After virus adsorption, DMEM containing 1 μg mL^{-1} of TPCK-treated trypsin, 0.14% BSA, 1.2% Avicel, and DMSO or test compounds was added to the cells. At 48 h post-infection, the cells were fixed with 4% formaldehyde and stained with 0.1% toluidine blue. Viral plaques were counted and the mean plaque number in the DMSO-treated control was set at 100%.

Biological evaluation (Flaviviruses and SARS-CoV-2)

Cells and viruses. The New Guinea C DENV serotype 2 strain and the WNV lineage 1 (Italy/2009) strain were kindly provided by the Istituto Superiore di Sanità (Rome, Italy) while the SARS-CoV-2 strain belonging to lineage B.1 (EPI_ISL_2472896) was kindly provided by the Department of Biomedical and Clinical Sciences Luigi Sacco, University of Milan (Italy). Once expanded in VERO E6 (African green monkey kidney cell line, ATCC catalog. n. CRL-1586), DENV, WNV and SARS-CoV-2 viral stocks were stored at −80 °C and titrated by the plaque assay, as previously described.[47]

The adherent human cell lines Huh7 (kindly provided by Istituto Toscano Tumori, Core Research Laboratory, Siena, Italy) and A549 ACE2-TMPRSS2(101006) were used to determine the cytotoxicity and the antiviral activity of candidate compounds against flaviviruses and SARS-CoV-2, respectively. Adherent cell lines were propagated in high glucose Dulbecco's Modified Eagle's Medium with sodium pyruvate and L-glutamine (DMEM; Euroclone) with 10% Fetal Bovine Serum (FBS; Euroclone) and 1% Penicillin/Streptomycin (Pen/Strep; Euroclone) used for Huh-7 or Minimum Essential Medium Eagle (EMEM; Euroclone) used for A549 supplemented with 10% Fetal Bovine Serum (FBS; Euroclone), 1% Penicillin/Streptomycin (Pen/Strep, Euroclone), 2 mM L-glutamine, 2 mg ml^{-1} G418 and 200 μg ml^{-1} of hygromycin B. For viral propagation, cytotoxic and antiviral experiments, a propagation medium with a lower concentration of FBS (1%) and 1% of Pen/Strep was used. The cells were incubated at 37 °C in a humidified incubator supplemented with 5% CO_2.

Cytotoxicity assay. The cytotoxicity of investigational compounds was determined by CellTiter-Glo 2.0 Luminescent Cell Viability Assay (Promega) according to the manufacturer's protocol. Cell viability was calculated by measuring cellular ATP as a marker of metabolically active cells through a luciferase-based chemical reaction. The luminescent signal obtained from cells treated with serial dilution of the investigational compounds, or DMSO as control, was measured using the GloMax® Discover Multimode Microplate Reader (Promega) and elaborated with the GraphPad PRISM software version 8.0 to calculate the half-maximal cytotoxic concentration (CC_{50}). Sofosbuvir (MCE® cat. HY-15005) and nirmatrelvir (NRM) used as reference compounds, were purchased from MedChem Express (**https://www.medchemexpress.com**) and

dissolved in 100% dimethyl sulfoxide (DMSO). Once determined, CC_{50}, for each compound chosen as a not-toxic dose, was used as the starting drug concentration in the subsequent antiviral.

Antiviral assays. To determine the antiviral activity of compounds against DENV, WNV and SARS-CoV-2, a direct yield reduction assay, based on the infection of cells in the presence of serial drug dilutions was performed as previously described with minor modifications.[47] Briefly, Huh7 or A549, pre-seeded in a 96-well format, were infected with viral stocks at a 0.005 multiplicity of infection (MOI). After 1 h of adsorption at 37 °C, the viral inoculum was removed and serial dilutions of each tested compound, starting from the not-toxic dose, were added to the infected cells. After 48 h of incubation for DENV and WNV and 96 h for SARS-CoV-2, the antiviral activity was measured on a cell monolayer by immunodetection assay (IA), as previously described[47,48] for DENV and WNV, and by CellTiter-Glo® Luminescent Cell Viability Assay evaluating the cytopathic effect (CPE) for SARS-CoV-2.[49]

The absorbance (expressed in OD450) for IA and the luminescence for CPE (expressed as RLU) were measured using the absorbance and the luminescence Module of the GloMax® Discover Multimode Microplate Reader (Promega). In each plate, the corresponding reference compound, the mock control (uninfected cells), the virus control and the virus back titration, performed diluting 2-fold the initial viral inoculum, were included. All drug concentrations were tested in duplicate in two independent experiments. In each plate, sofosbuvir and remdesivir were used as reference compounds against flaviviruses and SARS-CoV-2, respectively. Infected and uninfected cells without drugs were used to calculate 100% and 0% of viral replication, respectively. The half-maximal efficacy concentration (EC_{50}) was calculated through a non-linear regression analysis of the dose–response curves generated with GraphPad PRISM software version 8.0.

Author contributions

M. P., M. C. P., T. F., F. G., A. B., M. T. and C. B.: data curation, formal analysis, and investigation. M. L. B., R. G., V. C., I. V., O. T., M. Z. and A. L.: project administration and writing – review & editing. T. F. and S. M.: conceptualization, project administration, writing – original draft and writing – review & editing.

Conflicts of interest

There are no conflicts of interest to declare.

Acknowledgements

This work was supported by PRIN 2017 – cod. 2017BMK8JR (to T. Felicetti, I. Vicenti, M. Zazzi, V. Cecchetti, and S. Massari), PON "Ricerca e innovazione" 2014–2020, Azione IV.4 (tematiche dell'innovazione) – cod. J91B2100320006 (to T. Felicetti), Fondazione Umberto Veronesi – Post-doctoral Fellowships 2022 (to M. C. Pismataro), Associazione Italiana per la Ricerca sul Cancro, AIRC, grants IG 2016 – ID. 18855 and IG 2021 – ID. 25899 (to A. Loregian); Ministero dell'Istruzione, dell'Università e della Ricerca, PRIN 2017-cod. 2017KM79NN and PRIN 2022-cod. 20223RYYFC (to A. Loregian); Fondazione Cassa di Risparmio di Padova e Rovigo-Bando Ricerca Covid-2019 No. 55777 2020.0162-ARREST-COV: AntiviRal PROTAC-Enhanced Small-molecule Therapeutics against COronaViruses (to A. Loregian); EU funding within the NextGenerationEU-MUR PNRR Extended Partnership initiative on Emerging Infectious Diseases (Project No. PE00000007, INF-ACT) (to A. Loregian).

References

1 Q. Renyu, L. Yuchao, W. M. W. W. Kandegama, C. Qiong and Y. Guangfu, *Mini-Rev. Med. Chem.*, 2018, **18**, 781–793.
2 S. Pinheiro, E. M. C. Pinheiro, E. M. F. Muri, J. C. Pessôa, M. A. Cadorini and S. J. Greco, *Med. Chem. Res.*, 2020, **29**, 1751–1776.
3 M. A. Salem, M. S. Behalo and R. E. Khidre, *Mini-Rev. Org. Chem.*, 2021, **18**, 1134–1149.
4 T. Felicetti, M. C. Pismataro, V. Cecchetti, O. Tabarrini and S. Massari, *Curr. Med. Chem.*, 2021, **29**, 1379–1407.
5 R. Bivacqua, M. Barreca, V. Spanò, M. V. Raimondi, I. Romeo, S. Alcaro, G. Andrei, P. Barraja and A. Montalbano, *Eur. J. Med. Chem.*, 2023, **249**, 115136.
6 A. S. Abdelkhalek, M. Salah and M. A. Kamal, *Curr. Med. Chem.*, DOI: 10.2174/0929867330666230228120416.
7 S. Massari, G. Nannetti, J. Desantis, G. Muratore, S. Sabatini, G. Manfroni, B. Mercorelli, V. Cecchetti, G. Palù, G. Cruciani, A. Loregian, L. Goracci and O. Tabarrini, *J. Med. Chem.*, 2015, **58**, 3830–3842.
8 M. C. Pismataro, T. Felicetti, C. Bertagnin, M. G. Nizi, A. Bonomini, M. L. Barreca, V. Cecchetti, D. Jochmans, S. De Jonghe, J. Neyts, A. Loregian, O. Tabarrini and S. Massari, *Eur. J. Med. Chem.*, 2021, **221**, 113494.
9 S. Massari, C. Bertagnin, M. C. Pismataro, A. Donnadio, G. Nannetti, T. Felicetti, S. Di Bona, M. G. Nizi, L. Tensi, G. Manfroni, M. I. Loza, S. Sabatini, V. Cecchetti, J. Brea, L. Goracci, A. Loregian and O. Tabarrini, *Eur. J. Med. Chem.*, 2021, **209**, 112944.
10 J. Desantis, S. Massari, A. Corona, A. Astolfi, S. Sabatini, G. Manfroni, D. Palazzotti, V. Cecchetti, C. Pannecouque, E. Tramontano and O. Tabarrini, *Molecules*, 2020, **25**, 1183.
11 S. Massari, J. Desantis, G. Nannetti, S. Sabatini, S. Tortorella, L. Goracci, V. Cecchetti, A. Loregian and O. Tabarrini, *Org. Biomol. Chem.*, 2017, **15**, 7944–7955.
12 S. Imtiaz, J. A. War, S. Banoo and S. khan, *RSC Adv.*, 2021, **11**, 11083–11165.
13 Y. V. Sedash, N. Y. Gorobets, V. A. Chebanov, I. S. Konovalova, O. V. Shishkin and S. M. Desenko, *RSC Adv.*, 2012, **2**, 6719–6728.

14 G. Fischer, *Advances in Heterocyclic Chemistry*, Academic Press, 2019, vol. 128, pp. 1–101.
15 P. K. Singh, S. Choudhary, A. Kashyap, H. Verma, S. Kapil, M. Kumar, M. Arora and O. Silakari, *Bioorg. Chem.*, 2019, **88**, 102919.
16 A. Hibot, A. Oumessaoud, A. Hafid, M. Khouili and M. D. Pujol, *ChemistrySelect*, 2023, **8**, e202301654.
17 S. A. Komykhov, A. A. Bondarenko, V. I. Musatov, M. V. Diachkov, N. Y. Gorobets and S. M. Desenko, *Chem. Heterocycl. Compd.*, 2017, **53**, 378–380.
18 M. A. Kolosov, E. H. Shvets, D. A. Manuenkov, S. A. Vlasenko, I. V. Omelchenko, S. V. Shishkina and V. D. Orlov, *Tetrahedron Lett.*, 2017, **58**, 1207–1210.
19 S. Karami, M. Bayat, S. Nasri and F. Mirzaei, *Mol. Divers.*, 2021, **25**, 2053–2062.
20 M. A. A. Radwan, F. M. Alminderej, H. E. M. Tolan and H. M. Awad, *J. Appl. Pharm. Sci.*, 2020, **10**, 012–022.
21 V. M. Chernyshev, A. N. Sokolov and V. A. Taranushich, *Russ. J. Appl. Chem.*, 2007, **80**, 1691–1694.
22 Z. Zhang, Y. Pang, Y. Wang, C. Cohen, Y. Zhao and C. Liu, *Int. J. Antimicrob. Agents*, 2015, **45**, 491–495.
23 R. P. Brigance, W. Meng, A. Fura, T. Harrity, A. Wang, R. Zahler, M. S. Kirby and L. G. Hamann, *Bioorg. Med. Chem. Lett.*, 2010, **20**, 4395–4398.
24 D. A. Pyatakov, A. V. Astakhov, A. N. Sokolov, A. N. Fakhrutdinov, A. N. Fitch, V. B. Rybakov, V. M. V. V. Chernyshev and V. M. V. V. Chernyshev, *Tetrahedron Lett.*, 2017, **58**, 748–754.
25 P. P. Warekar, P. T. Patil, K. T. Patil, D. K. Jamale, G. B. Kolekar and P. V. Anbhule, *Synth. Commun.*, 2016, **46**, 2022–2030.
26 Y. M. Ren and C. Cai, *Monatsh. Chem.*, 2009, **140**, 49–52.
27 K. V. N. S. Srinivas and B. Das, *Synthesis*, 2004, **2004**, 2091–2093.
28 L. Brinchi, R. Germani, G. Savelli and D. Biondini, *Lett. Org. Chem.*, 2006, **3**, 207–211.
29 V. M. Chernyshev, A. N. Sokolov and V. A. Taranushich, *Russ. J. Appl. Chem.*, 2006, **79**, 1134–1137.
30 H. Nagarajaiah, A. Mukhopadhyay and J. N. Moorthy, *Tetrahedron Lett.*, 2016, **57**, 5135–5149.
31 C. O. Kappe, *J. Org. Chem.*, 1997, **62**, 7201–7204.
32 K. S. Atwal, G. C. Rovnyak, B. C. O'Reilly and J. Schwartz, *J. Org. Chem.*, 1989, **54**, 5898–5907.
33 C. O. Kappe, *Acc. Chem. Res.*, 2000, **33**, 879–888.
34 X. Huo, Y. Ma, Z. Chen, L. Yuan, X. Zheng, X. Li, F. Liang, W. You and P. Zhao, *ChemistrySelect*, 2021, **6**, 4562–4565.
35 N. Khetarpal and I. Khanna, *J. Immunol. Res.*, 2016, **2016**, 6803098.
36 Dengue—Level 3 cause | Institute for Health Metrics and Evaluation, **https://www.healthdata.org/results/gbd_summaries/2019/dengue-level-3-cause**, (accessed 16 October 2021).
37 X. Yang, M. B. M. Quam, T. Zhang and S. Sang, *J. Travel Med.*, 2021, **28**, 146.
38 G. Habarugira, W. W. Suen, J. Hobson-Peters, R. A. Hall and H. Bielefeldt-Ohmann, *Pathogens*, 2020, **9**, 1–51.
39 R. Lu, X. Zhao, J. Li, P. Niu, B. Yang, H. Wu, W. Wang, H. Song, B. Huang, N. Zhu, Y. Bi, X. Ma, F. Zhan, L. Wang, T. Hu, H. Zhou, Z. Hu, W. Zhou, L. Zhao, J. Chen, Y. Meng, J. Wang, Y. Lin, J. Yuan, Z. Xie, J. Ma, W. J. Liu, D. Wang, W. Xu, E. C. Holmes, G. F. Gao, G. Wu, W. Chen, W. Shi and W. Tan, *Lancet*, 2020, **395**, 565–574.
40 C. B. Jackson, M. Farzan, B. Chen and H. Choe, *Nat. Rev. Mol. Cell Biol.*, 2022, **23**, 3–20.
41 S. Fawell, J. Seery, Y. Daikh, C. Moore, L. L. Chen, B. Pepinsky and J. Barsoum, *Proc. Natl. Acad. Sci. U. S. A.*, 1994, **91**, 664–668.
42 G. Muratore, L. Goracci, B. Mercorelli, Á. Foeglein, P. Digard, G. Cruciani, G. Palù and A. Loregian, *Proc. Natl. Acad. Sci. U. S. A.*, 2012, **109**, 6247–6252.
43 I. D'Agostino, I. Giacchello, G. Nannetti, A. L. Fallacara, D. Deodato, F. Musumeci, G. Grossi, G. Palù, Y. Cau, I. M. Trist, A. Loregian, S. Schenone and M. Botta, *Eur. J. Med. Chem.*, 2018, **157**, 743–758.
44 A. Loregian, B. A. Appleton, J. M. Hogle and D. M. Coen, *J. Virol.*, 2004, **78**, 158–167.
45 A. Loregian and D. M. Coen, *Chem. Biol.*, 2006, **13**, 191–200.
46 G. Nannetti, S. Massari, B. Mercorelli, C. Bertagnin, J. Desantis, G. Palù, O. Tabarrini and A. Loregian, *Antiviral Res.*, 2019, **165**, 55–64.
47 I. Vicenti, M. G. Martina, A. Boccuto, M. De Angelis, G. Giavarini, F. Dragoni, S. Marchi, C. M. Trombetta, E. Crespan, G. Maga, C. Eydoux, E. Decroly, E. Montomoli, L. Nencioni, M. Zazzi and M. Radi, *Eur. J. Med. Chem.*, 2021, **224**, 113683.
48 M. G. Martina, I. Vicenti, L. Bauer, E. Crespan, E. Rango, A. Boccuto, N. Olivieri, M. Incerti, M. Zwaagstra, M. Allodi, S. Bertoni, E. Dreassi, M. Zazzi, F. J. M. van Kuppeveld, G. Maga and M. Radi, *ChemMedChem*, 2021, **16**, 3548–3552.
49 L. Fiaschi, F. Dragoni, E. Schiaroli, A. Bergna, B. Rossetti, F. Giammarino, C. Biba, A. Gidari, A. Lai, C. Nencioni, D. Francisci, M. Zazzi and I. Vicenti, *Viruses*, 2022, **14**, 1374.